NASA CONTRACTOR REPORT

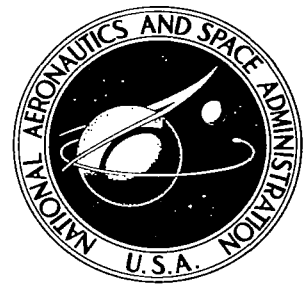

N.A.S.A. C.R. 388

NASA CR-388

REACTION WHEEL WITH BRUSHLESS DC MOTOR DRIVE

by W. M. Casaday

Prepared under Contract No. NAS 5-9016 *by*
SPERRY FARRAGUT COMPANY
Bristol, Tenn.
for Goddard Space Flight Center

NATIONAL AERONAUTICS AND SPACE ADMINISTRATION • WASHINGTON, D. C. • APRIL 1966

NASA CR-388

REACTION WHEEL WITH BRUSHLESS DC MOTOR DRIVE

By W. M. Casaday

Prepared under Contract No. NAS 5-9016 by
SPERRY FARRAGUT COMPANY
Bristol, Tenn.

for Goddard Space Flight Center

NATIONAL AERONAUTICS AND SPACE ADMINISTRATION

For sale by the Clearinghouse for Federal Scientific and Technical Information
Springfield, Virginia 22151 – Price $0.95

SECTION I

SUMMARY

A. OBJECT

This final report describes a program sponsored by the National Aeronautics and Space Administration's Goddard Space Flight Center to design, develop, and manufacture four reliable, efficient, lightweight, sealed brushless DC reaction wheel systems. These systems are described in Goddard Space Flight Center (GSFC) Specification 67-33 dated 4 March 1964 and revised 29 January 1965.

In these motors photo-optical detectors and transistorized switches perform the functions of a conventional commutator without physical contact between the commutator and armature. The principles of operation of a brushless DC motor as developed by Sperry Farragut Company (SFCo) are well known to GSFC and are explained in the final report for contract NAS 5-3582.

B. SCOPE

This report covers the entire contract period and describes the design, development, and manufacture of the four reaction wheels and discusses the achieved characteristics. The original specification which called for four identical units was revised to specify three different systems as described below:

1. Two units (hereafter referred to as units one and two) to have constant torque of 0.5 ft. lb. to 250 RPM and capability of accelerating to 1000 RPM.
2. One unit (unit three) to have constant torque of 0.625 ft. lb. from 0 to 250 RPM.
3. One unit (unit four) to have constant torque of 0.125 ft. lb. from 0 to 500 RPM.

C. CONCLUSIONS

The state-of-the-art in attitude control using inertia wheels has been significantly increased by the development of these reaction wheels driven by brushless DC motors. A survey made by NASA/GSFC indicates that these reaction wheels provide more inertia per pound than systems that are currently being used for satellite attitude control. See Figure 1. Reliability has been increased by eliminating sliding contact brushes and their associated problems. Heat transfer is greatly improved since the armature winding is stationary and mounted directly to the case. Bearing reliability is increased since no heat is generated in the rotating assembly. Regenerative braking has been incorporated in units three and four which use the voltage generated in the armature windings to give complete control of the rotating wheel while it is decelerating.

D. RECOMMENDATIONS

The following recommendations are made by SFCo to further develop the state-of-the-art in reaction wheels by increasing performance and reliability and decreasing weight and size.

The ripple torque for unit three was measured to be ±8.9 percent of which the theoretical ripple due to commutation was ±7.2 percent using the three segmented commutator. SFCo recommends using a five-segment commutator which has ±2.5 percent theoretical torque ripple due to commutation. The predicted torque ripple of the system is ±4.2 percent which is a significant reduction. Also, in the event of a switch failure, the motor would continue to run and the performance would be reduced only approximately 10 percent. The motor would still start in any position.

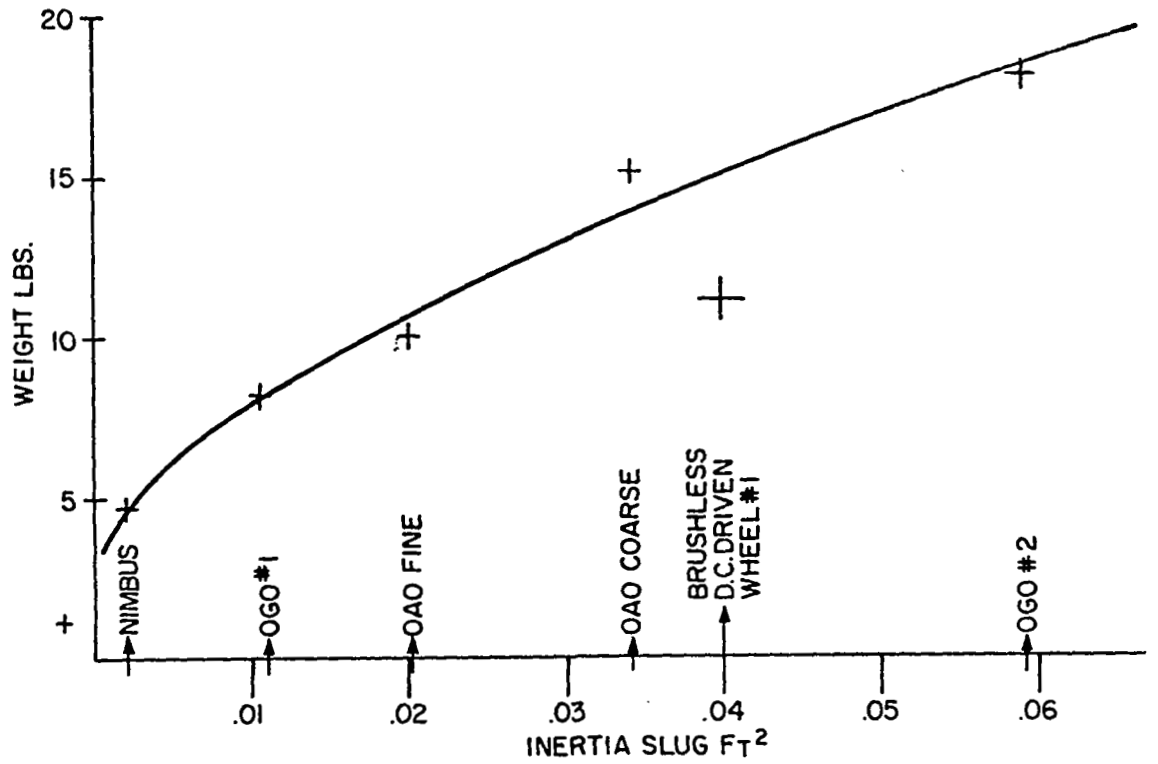

FIGURE 1
REACTION WHEEL WEIGHTS

SFCo recommends further investigation of the ironless motor concept discussed in this report. The ironless approach will result in a lighter system, lower friction torque, and high efficiency.

SECTION II

STATEMENT OF WORK

A. SCOPE

Sperry Farragut Company (SFCo) was to furnish the necessary personnel, facilities, services, and material to design, develop, fabricate, and deliver to Goddard Space Flight Center (GSFC) four reaction wheel systems driven by brushless DC motors.

B. TECHNICAL REQUIREMENTS FOR UNITS ONE AND TWO

The following are the original technical contract requirements for units one and two.

1. Operational Parameters
   a. Inertia - 1.25 lb. ft.^{2}
   b. Angular Momentum - 1.0 lb. ft. sec. @ 250 RPM
   c. Torque - 0.5 ft. lb. (0 to 250 RPM)
   d. Speed - 1000 RPM max.
   e. Power Input - 30 watts max.
   f. Voltage - 24 VDC
   g. Weight - 10 lb. max.
   h. Size - 12" x 12" x 4"
   i. Ripple-torque - ±5% of output
2. Mechanical Limitations
   a. Friction - 0.005 ft. lb. max.
   b. Hermetic Sealing - The device must be capable of operation with an internal pressure of 0.01 mm. Hg.

3. Electrical Limitations

a. Control Input

(1) The device must be capable of providing a constant torque with a linearity of ±5% when controlled with a pulse width modulated input signal varying from 3% to 97% from 0 to 250 RPM.

(2) The torque motor must be capable of accelerating the wheel at a lower torque level to a maximum speed of 1000 RPM.

(3) An electrical signal proportional to wheel velocity within 5% must be available.

b. Reversibility - The device must respond in either direction at any angular position of the wheel depending on the polarity of the input signal.

c. Electronic Commutator - The commutation circuitry shall not require more than 10% of the input power at any operating point.

4. General

a. Reliability - Based on accepted failure rate criteria a 92% reliability for a lifetime of 3 years at an average power level of 10% is required.

b. Environmental Conditions - The device must be capable of operating during and after 50 g shock of 2 ms duration and 5 minutes of 15 g rms random vibration in each of three perpendicular planes and at temperatures of $-10^{o}C$ to $+70^{o}C$.

C. SPECIFICATION CHANGES FOR UNITS ONE AND TWO

The following electrical limitations were made to the technical specifications at the direction of or with the consent of GSFC:

1. Control Input

The pulse width modulation control was changed to a DC voltage control.

The device is capable of providing a constant torque with a linearity of ±5% when controlled by a 0 to +12 volt DC signal.

2. Reversibility

   Two +24 volt command signals were provided to control the direction of rotation.

3. The environmental specification was changed to eliminate the requirement for units one and two to operate during shock and vibration. It was also agreed that shock and vibration tests would be run only on production unit three or four.

4. It was requested that the commutating electronics for units one and two be mounted externally on the reaction wheel housing and that the devices not be hermetically sealed.

D. TECHNICAL REQUIREMENTS FOR UNITS THREE AND FOUR

The following are the requirements of Specification 67-33, Revision A for units three and four:

1. Operational Parameters
   a. Inertia - 1.25 lb. ft.^{2}
   b. Angular Momentum - 1.0 lb. ft. sec. @ 250 RPM.
   c. Torque
      (1) 0.625 ft. lb. (0 to 250 RPM) - Unit 3
      (2) 0.125 ft. lb. (0 to 500 RPM) - Unit 4
   d. Power Input
      (1) 30 watts max. - (Unit 3)
      (2) 16 watts max. - (Unit 4)
   e. Voltage - 21-36 VDC
      24 ±1 VDC

f. Weight - 12 lb. max.

g. Size - 12" x 12" x 4"

h. Ripple torque - ±5% output

2. Mechanical Limitations

a. Friction - 0. 005 ft. lb.

b. Hermetic Sealing - The device must be capable of operation with an internal pressure of 0. 01 mm Hg and structurally able to withstand 1/2 atmospheric differential pressure. An internal pressure as high as 1/2 atmospheric pressure may be used.

3. Electrical Limitations

a. Control Input

(1) The device must be capable of providing a constant torque with a linearity of ±5% when controlled by a pulse width modulated signal from zero to unload speed when supplied with a 24-volt source.

(2) The above control signal requirement shall not exceed 4 volts nor be required to have an impedance less than 1, 000 ohms.

(3) An electrical signal proportional to wheel velocity within 5% must be available. This signal shall be at least 10 volts at the unload speed with an output impedance not greater than 10, 000 ohms.

b. Reversibility

(1) The torque direction response shall be a function of which one of two control inputs is supplied with a signal.

(2) These signals shall not be required to be greater than 4 volts nor have an impedance less than 1, 000 ohms.

c. Electronic Commutator - The commutator circuitry shall not require more than 10% of the input power or 2 watts, whichever is greater.

d. Dynamic Braking - Whenever deceleration of the wheel is required and the internally generated voltage is sufficient to provide enough current to the load, the device shall respond as specified without using more external source power than required for commutation and control circuitry.

4. General

The reliability and environmental conditions are the same as for units one and two.

E. SPECIFICATION CHANGES FOR UNITS THREE AND FOUR

The following changes were made to the technical specification at the direction of or with the consent of GSFC:

1. Operational Parameters

An additional voltage of -14 VDC was supplied.

2. Electrical Limitations

The pulse width modulation control was changed to a DC voltage control. The device is capable of providing a constant torque with a linearity of ±5% when controlled by a zero to 4 volt DC signal.

3. The environmental specification was changed to eliminate the requirement for the unit to operate during shock and vibration.

SECTION III

PERFORMANCE OF WORK

A. MOTOR DEVELOPMENT

At the request of GSFC two approaches to the motor design were analytically evaluated. These approaches were the torquer concept and the ironless motor concept. Explanation of these two approaches follows:

1. Torquer Concept

The torquer design is the standard mechanical configuration for a pancake motor with a winding to permit electronic commutation. In the usual winding method an even number of slots per pole pair was used. After it was determined that an odd number of slots per pole pair could be properly wound, 63 stator slots were used to materially reduce cogging torque.

Vanadium Permendur was chosen for the stator material because it has a saturation density greater than silicon steel.

Two motor windings were used to provide the wheel velocity range desired. The 250 RPM winding was used to provide the 0.5 ft. lbs. of torque from 0-250 RPM and a 1000 RPM winding was used to provide the capability of accelerating the wheel at a lower torque level up to 1000 RPM. The 250 RPM winding occupies 75% of the available slot space and the 1000 RPM winding occupies 25 percent. The motor design characteristics are described below.

a. 250 RPM Winding

Back EMF - $5.45\ n \times 10^{-2}$; n = RPM

Resistance - 3.07 ohms

Torque - 0.5 ft. lb. from 0 to 250 RPM

Voltage - 24 VDC

Current - 1.25 amperes

b. 1000 RPM Winding

Back EMF - $1.36\ n \times 10^{-2}$

Resistance - 0.61 ohms

No load speed - 1000 RPM

Voltage - 24 VDC

Current - 1.25 amperes

2. Ironless Motor Concept

At the suggestion of GSFC, a motor was investigated using the ironless (printed-circuit) motor concept. The field circuit rotates and provides the major portion of the required inertia. A printed-circuit stator was not practical due to the limited number of conductors possible. A card was designed to determine the feasibility of the configuration. Two main advantages result from the ironless-motor concept. The majority of the motor weight is used to provide the inertia, thus reducing over-all motor weight. Also, the friction torque is quite small since no magnetic material is present in the wound member. For this reason, the efficiency of such a motor would be higher than what could be achieved with the torquer design.

Original plans were to build a breadboard ironless motor and evaluate it along with a breadboard torquer. A decision was made by GSFC, however, not to proceed with the ironless approach under this contract. Sperry Farragut has submitted an unsolicited proposal to GSFC to design, develop, and fabricate a brushless DC motor driven reaction wheel using the ironless technique.

3. Production Units

A breadboard reaction wheel system was fabricated and evaluated. The breadboard model performance was analyzed and used as the basis for the motor design for the four production units. The breadboard motor produced a high cogging torque due to a sudden flux change as the stator tooth entered the main flux field. The production units utilized a skewed stator to permit a gradual flux change as each tooth enters the main flux field and thus reduced the cogging torque. The ripple torque due to cogging in the breadboard motor was ±10.25 percent. By skewing the stator, the cogging torque was reduced to ±5.8 percent in units one and two. A stator change involving a different number of teeth and a different winding configuration was made in units three and four which further reduced the cogging torque to less than ±1.5 percent. This stator change is explained in the following paragraphs.

For a standard wave winding in a typical brush-type torquer, the number of teeth are found by multiplying the number of poles selected by an integer (usually 5) and adding one tooth (progressive winding) or subtracting one tooth (retrogressive winding). For example, a six pole torquer may have $6 \times 5 + 1 = 31$ teeth, or $6 \times 5 - 1 = 29$ teeth. This combination of poles and number of teeth automatically results in the most desirable conditions for minimum ripple torque. Since the poles are equally spaced around the periphery, every tooth is positioned differently in the main flux field. The ripple torque produced by a tooth entering or leaving the main flux field is minimized since the ripple torque produced by any tooth is not directly

additive to that produced by any other tooth. The frequency of this cogging torque is the number of teeth multiplied by the number of poles.

In the SFCo method of brushless commutation, it is desirable for simplicity of design and winding to use an even number of teeth. However, this results in high ripple torque due to addition of the ripple from several teeth. For example, in the 6 pole torquer described above, 30 teeth may be used. This would result in a ripple torque 6 times as great as 31 teeth would produce since a tooth would be entering the flux field of every pole at the same instant. To eliminate this problem, SFCo has designed, tested, and proven a modified distributed winding which permits the use of a fractional number of teeth per pole and reduces the ripple due to cogging to the level presently obtained with brush-type torquers.

Units one and two used 63 tooth stators with the 14 pole rotor. This created a cogging condition where an identical tooth placement was under a pair of poles at any instant (nine teeth per pole pair). Thus, seven teeth contributed to the cogging torque. With 65 teeth, no two teeth in the stator are in the same position with respect to any of the main flux fields. Units three and four contained 65 tooth stators, and a cogging torque reduction of 7 to 1 was realized.

B. COMMUTATOR

The photo-electronic commutator for the reaction wheel system utilizes the same basic principles described in the final report on Contract NAS 5-3582.

The use of a fourteen pole motor to drive the inertia wheel necessitated the solid state commutator to go through a complete electrical switching cycle in one seventh of a mechanical revolution of the wheel, or seven complete cycles in one revolution

of the wheel. To provide this switching capability, the photosensors were equally spaced around the periphery of a sensor holder and a separate light source used to illuminate each sensor. A symmetrical light shield with seven slots rotates between the light sources and the sensors to illuminate each photosensor seven times per revolution of the wheel. The photosensors are located on a large diameter to provide faster switching speed. Spacing the photosensors equally around the periphery of the sensor holder eliminated mutual coupling by light reflections from the rotating shield. The configuration of the light chopper and the layout of the lamps and sensors can be seen in Figure 2.

The mechanical complexity of the system made the normal method of using one lamp to illuminate the six sensors impractical.

1. The commutator for units one and two is shown in SFCo drawing, ENG 10084, "Schematic for Reaction Wheels 1 & 2." CR13, 14, and 15 prevent breakdown of transistors Q4, Q5, and Q6 when the motor is reversed by blocking the high developed voltage. CR16, 17, & 18 prevent breakdown of transistors Q13, Q14, and Q15. K1, a latching relay, is used to switch the system from the 250 RPM mode of operation to the 1000 RPM mode.

2. The commutator for units three and four is shown in ENG 10131 and in Figure 3 of the monthly progress report for May, 1965. This circuit is designed to operate over an applied voltage range of 21-36 VDC. Those components shown in dotted lines in Figure 3 of the progress report are the additional components necessary to incorporate regenerative braking which will be discussed in a later section.

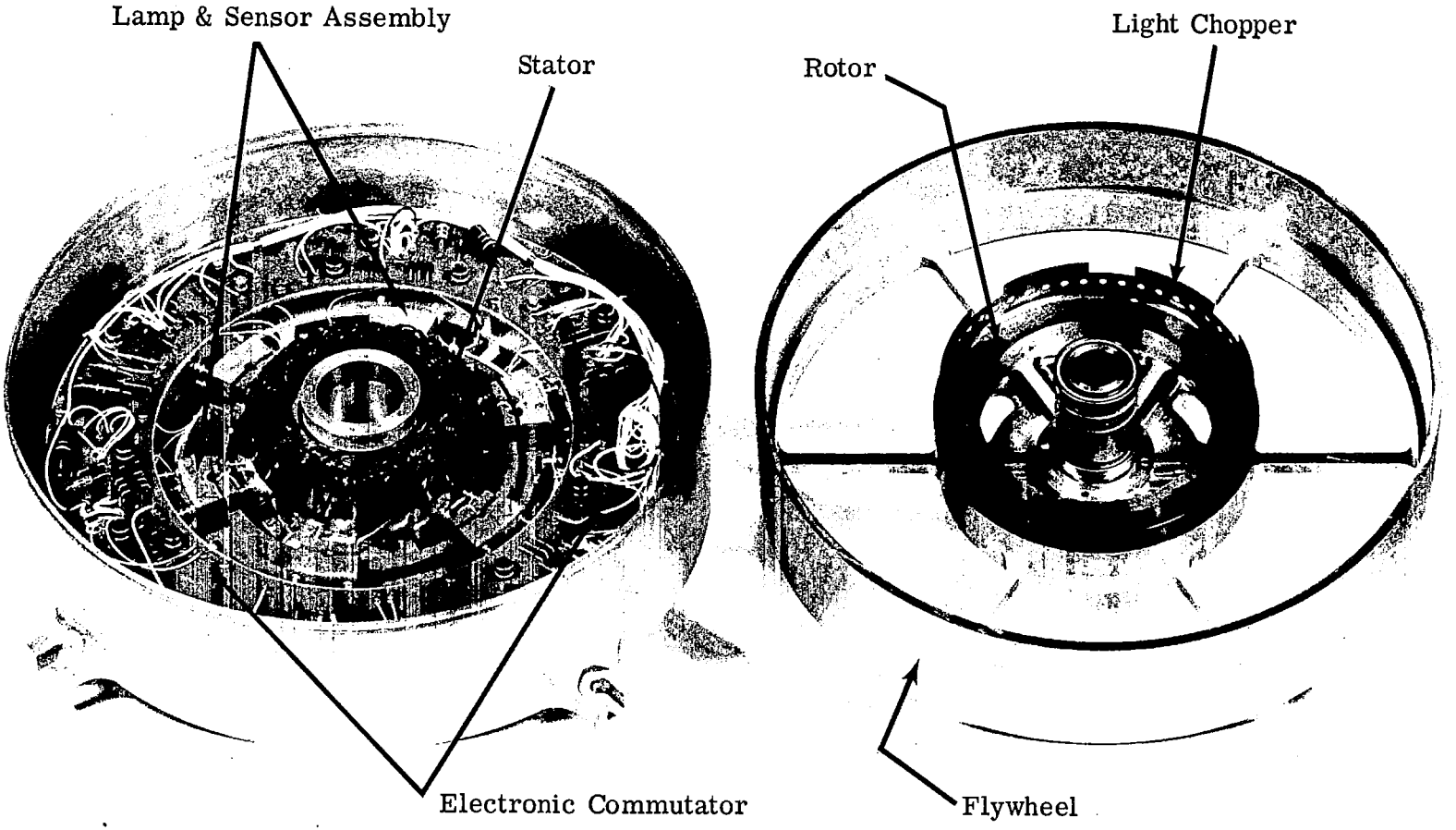

FIGURE 2.
REACTION WHEEL WITH FLYWHEEL REMOVED

The commutator for unit four is the same as that for unit three except for some resistance changes necessitated by lower current requirements for unit four. In Units one and two, a diode was used in series with each upper switch to prevent breakdown of the upper switches when the motor was reversed. For units three and four the motor is to go into the regenerative braking mode where it will stay until the generated voltage is insufficient to provide the required current. Then the motor goes into the driving mode at which time the generated voltage will be low enough so that the output transistors in the upper switches will not break down. If the regenerative braking circuit ever failed, some protection might be required for the transistors to insure that the motor could still perform satisfactorily. This protection was provided by replacing the upper switch Darlington resistor with a diode. Switch 4, for example, protects transistor Q34. To insure that the emitter-base junctions of Q33 and Q34 do not break down together, diode CR98 and Zener diode CR99 were placed across Q34 to keep the emitter of Q34 from going more than approximately 16 volts more positive than the collector. It would take approximately 22 volts to break down both junctions in series. The voltage divider action of R103 and R134 limits the voltage across each junction to a safe value of approximately 7.5 volts.

Diodes CR44, CR58, and CR31 clamp the bases of Q32, Q39, and Q25 and thus set a maximum on the pre-amp currents that can flow as the voltage varies from 21-36 VDC.

3. The lamp circuit shown in Figure 3 of the May progress report uses an NPN transistor Q18 and a 21-volt Zener diode to regulate the voltage to the 7 series

lamps. The data shown below shows how the lamp voltage and circuit currents changed as the supply voltage was varied from 21 to 36 VDC.

Supply Voltage VDC	V_1 VDC	V_2 VDC	I_1 M. A.	I_2 M. A.	I_3 M. A.	I_4 M. A.
21	19.81	2.77	38	38.5		
24	20.86	2.92	39.5	35	5	2.55
30	21.37	3.006	40	22.5	17	7.6
36	21.91	3.083	40.5	10	30	13

When the supply voltage is 36 VDC most of the lamp current flows through R11, thus the dissipation in Q18 is decreased. I_2 should be shown as the emitter current instead of the base current.

C. PULSE WIDTH MODULATION (PWM)

The specification originally required a linear variation of output torque from 0 to unload speed when controlled by a pulse width modulated signal. The peak armature current was to be limited to a specified value which would vary the average armature current as the width of the applied voltage pulse varied. The circuit shown in Figure 1 of the progress report for September, 1964 was used to provide PWM control. Photosensors A2, A4, and A6 will conduct when light impinges upon them. The pre-amp transistors Q1, Q4, and Q7, however, can not conduct until a ground path is provided through transistor Q_A. The pre-amp current through Q1, Q4, and Q7 then is modulated resulting in the armature current being modulated. The lower switches (one, three and five) will not be modulated since one of the upper switches will be on at all times and will provide the modulation. Using this method of modulation, with the armature current limited to 1.4 amperes, the reaction

wheel stall torque was measured at various percentages of modulation. The data shown below was plotted in Figure 3 of this report.

PWM (%)	Line Current (Amps)	Torque (Ft. Lbs.)
10	.195	.087
15	.305	.188
20	.47	.322
40	.71	.38
60	1.01	.419
75	1.21	.433
84	1.34	.443

This curve was supposed to be linear within ±5% but was not. The reason the curve was not linear is that a very high time constant exists in this motor due to the high inductance of the windings and the low impedance of the commutating transistors while the current is not being limited. At low percentages of PWM the time constant of the windings and current limiter is higher than the width of the pulse so the current limiter did not limit to 1.4 amp pulses. The current would never reach 1.4 amps until the width of the pulse exceeded the time constant of the windings. Thus, at higher percentages of PWM the curve became more linear. The same current limiting circuit was used to run the motor with a PWM frequency of 500 cps and 5000 cps by modulating first the upper switches, then the lower switches, and finally both sets of switches together. The same shape curve resulted for all sets of conditions. It did not appear feasible to use a system of PWM control for a motor of this type with current limiting. With the approval of GSFC, SFCo then developed a method of providing a linear torque variation by varying the level of the armature current rather than the ratio of "on" time to "off" time provided by PWM. This concept is explained in the following section on current limiting.

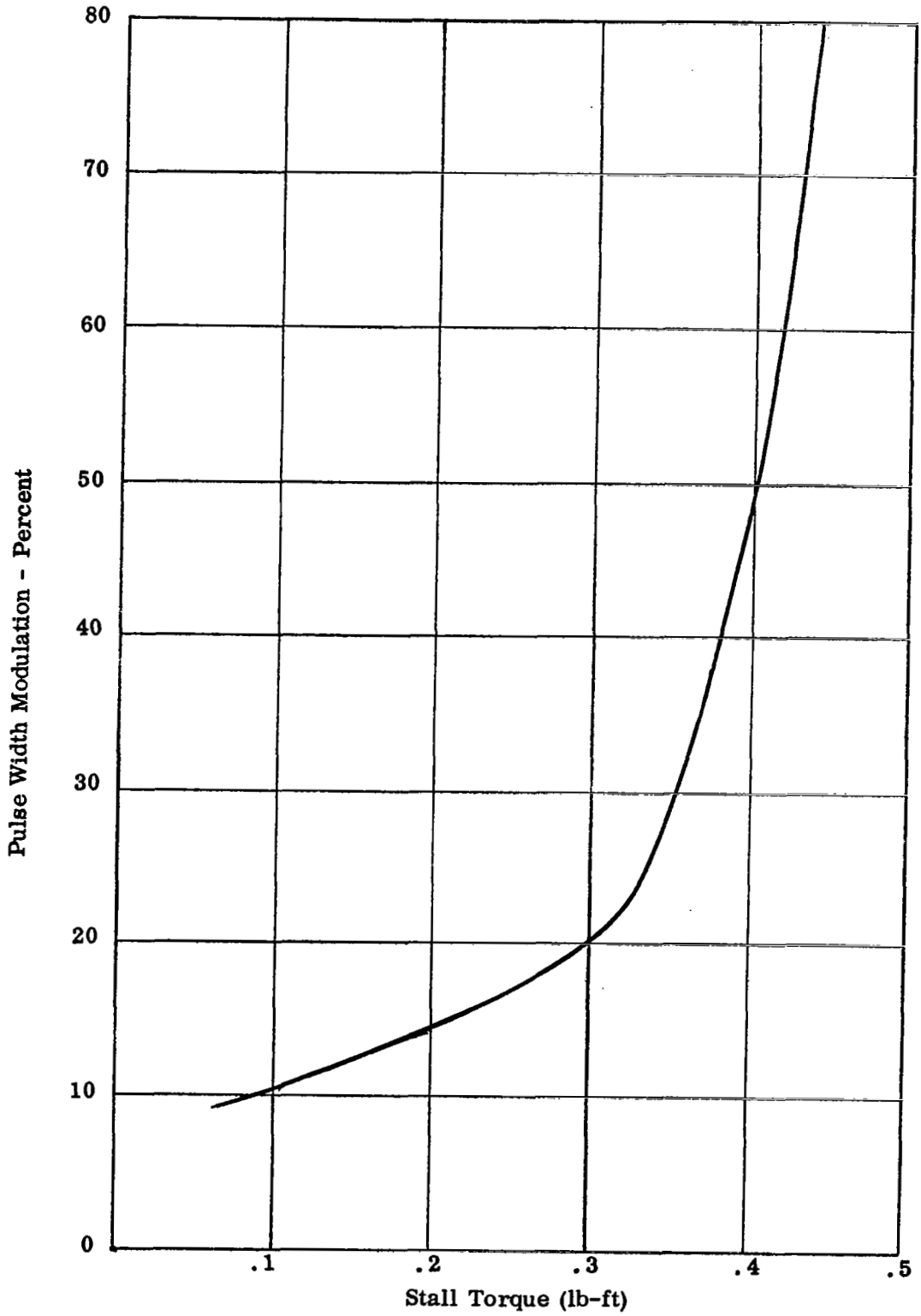

FIGURE 3
STALL TORQUE VS. PWM

D. CURRENT LIMITING

The constant torque characteristic desired in the reaction wheel systems was obtained by limiting the armature current to the value needed to produce the specified torque at the specified speed. Several methods of current limiting were investigated.

1. Series Limiter

The first limiting scheme investigated was placing one current limiting transistor in series with the commutator and the ground return as shown in Figures 1a and 2a in the progress report for September, 1964. In Figure 2a, the base current of Q7 is set by selecting RX so that by transistor action, Q7 will limit the motor current to 1.4 amperes. With this configuration the current limiter would be connected to the emitters of all three of the lower output switches (1, 3, and 5) and thus would have to handle all of the motor current. This circuit was ruled out by the requirement that the reaction wheel must be reversible. The voltage across the winding (simulated by R_w) goes to about 46 volts when the motor is reversed while running at a speed near its no load speed. When this occurs, the current limiter (Q7) has to develop approximately 40 volts from collector to emitter to limit the current to 1.4 amperes. This places a 40-volt potential on the emitter of Q6 and turns Q6 off since all pre-amp currents originate from a 24-volt supply. This type of current limiting was not appropriate.

2. Integrated Limiter

The second limiter circuit investigated was to replace the output transistors of the lower switches (1, 3, and 5) with higher power transistors and let each of these output transistors be a current limiter in itself as shown in Figures 1c and 2c of the September, 1964 progress report. In the circuit shown in Figure 2c, the current through each output transistor Q5 can be

set to provide the proper base drive to Q5. Since these same limiting transistors are being used as the commutating switches, additional power to drive the current limiter is not required as it is in other current limiting techniques. By integrating the current limiting function into the commutator, the requirement for adding a separate series limiter with its intrinsic characteristics of reducing reliability was eliminated. The transistors chosen are capable of 100 watts dissipation at a case temperature of 100°C and are capable of operating continuously with the wheel in the stall condition. However, during normal operation, each switch has a 33-1/2% duty cycle thus reducing the dissipation in each transistor and further increasing reliability.

The integrated current limiting approach was chosen but the simple circuit of Figure 2c was not stable enough with variations in temperature due to the dependence upon the DC beta of the transistors. The following circuits were investigated as a means of providing better current control:

a. Nickel Cadmium Battery Limiter - The current limiting circuit shown in Figure 1 in the progress report for December, 1964 was breadboarded and tested. The current limiting transistors are used as the output transistors of the lower switches as in the initial current limiting circuits. Resistor R3 is common for all three limiting transistors as is the nickel cadmium battery. The circuit functions as follows: The voltage on the current limiter transistor base cannot go above the battery voltage plus the drop across CR1. R3 is selected to give the desired emitter current with the constant base voltage. If the current through R3 tries to increase, the emitter voltage of the limiting transistor increases to a value that causes the limiter transistor

to try to cut off, thus, the current is limited to the selected value. A disadvantage of this circuit is the additional power dissipated in R3.

In this circuit the nickel cadmium battery is being charged when the current is being limited and the only drain from the battery is that allowed through the reverse impedance of the three diodes (one for each switch). The diodes serve as temperature compensation for the base-emitter junction of the limiting transistors as well as preventing battery drain. The breadboard reaction wheel was run with this current limiting to evaluate the current limiting from $-15^{o}C$ to $+75^{o}C$, with the current plotted against speed as shown in Figure 4 of this report. The armature current varied approximately ±50 ma from $-15^{o}C$ to $+75^{o}C$.

This current limiting circuit was not incorporated because of the temperature limitation of nickel cadmium batteries. The battery life dropped to about 400-500 hours at an ambient temperature of $70^{o}C$ compared to a life of several years at temperatures up to $60^{o}C$.

b. Zener Diode Limiter - A brief investigation was made concerning the use of a temperature compensated zener diode with a sharp knee to replace the nickel cadmium battery. This technique was not investigated thoroughly since the problem of nonlinearity of torque versus Pulse Width Modulation necessitated switching to a current limiter which could be controlled by a varying DC voltage.

c. DC Controlled Current Limiting - A circuit diagram of the DC controlled current limiting is shown in ENG 10084, the schematic diagram of units one and two. Operation of the circuit is as follows: Resistor R38 is

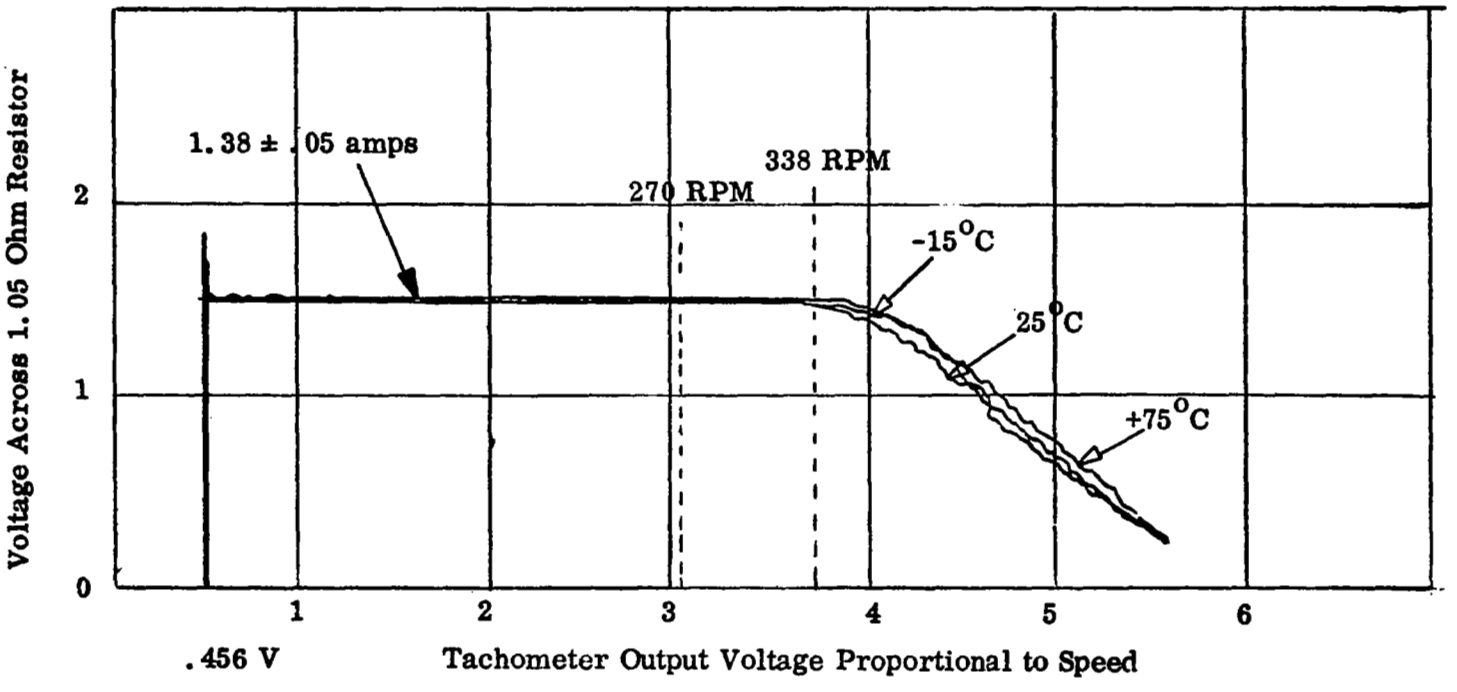

FIGURE 4
CURRENT LIMITER PERFORMANCE

selected sufficiently small such that with a control voltage input of zero volts, almost all of the current through R22 flows through CR25, CR28, and R38 and the resulting voltage on the base of Q10 is insufficient to cause Q13 to conduct although some current may flow through R29. As the control voltage increases, the base of Q10 becomes more positive and Q10 conducts more, causing Q13 to conduct and armature current to flow. The base voltage of Q13 can not go above a value determined by the forward voltages of CR25 and CR28 and the current flowing through R38. Thus the voltage at the emitter of Q13 is limited to the base voltage of Q10 less the summation of base-emitter drops on Q10 and Q13, i.e., $V_{E13} = V_{B10} - (V_{BE10} + V_{BE13})$. The armature current is limited to $I = V_{E13}/R_{37}$. As the motor speed falls below 250 RPM, the counter emf decreases and the armature current tries to increase, but it raises the voltage on the emitter of Q13 and tends to reverse bias the base emitter junction and turn Q13 off. This type of current limiter does not depend upon the DC Beta of Q13 as long as R18 is selected to provide enough base current to saturate Q13 when the armature current is approaching the limiting value and limiting is not required. Resistor R18 can be selected such that an upper limit is held on the current by the DC Beta of Q13 regardless of how high the control input voltage might go. Diodes CR25 and CR28 provide temperature compensation for the change in base-emitter voltages of Q10 and Q13. The DC control voltage is applied to a pure resistive voltage divider and gives linear variation of torque versus control voltage within 5 percent. The control input voltage divider and the sensing resistor R37 are common to all three current

limiters. Controlling the torque by varying the armature current with the DC control voltage allows the reaction wheel system to operate as a constant torque device at torque levels between 0 and the rated torque of the BDCM. The first two reaction wheels (units 1 and 2) had an open loop current control circuit as shown in the schematic. A differential amplifier was included in units 3 and 4 to provide a high gain closed loop control of the current limiter.

E. DIRECTION OF ROTATION DETECTOR

The direction of motor rotation is determined by detecting the sequence in which a pair of photosensors is energized. The direction sensing system includes a light source, a 50 slot tone wheel (light chopper), two photosensors and the circuitry shown in block diagram form in Figure 5. The tone wheel direction of rotation is sensed as each slot passes between the light source and the photosensors. When the light strikes the first sensor, its output increases until the flip-flop (FF) is set to the state corresponding to that particular sensor. The output of the sensor increases further until the upper trigger point (UTP) of the Schmitt trigger is reached. This clamps the sensor inputs to the FF. The sensors are spaced relative to each other so that the voltage output from the first one subjected to the light has reached the Schmitt UTP before the other has reached the FF trigger level. However, they must be close enough so that both sensor outputs are above the Schmitt lower trigger point (LTP) for some instant as the light beam sweeps across them. This keeps the sensor inputs clamped to the FF. Since the FF trigger voltage is between the UTP and LTP, the FF inputs remain clamped until the output voltage of both sensors has decreased below the LTP of the Schmitt. When no light is incident on the

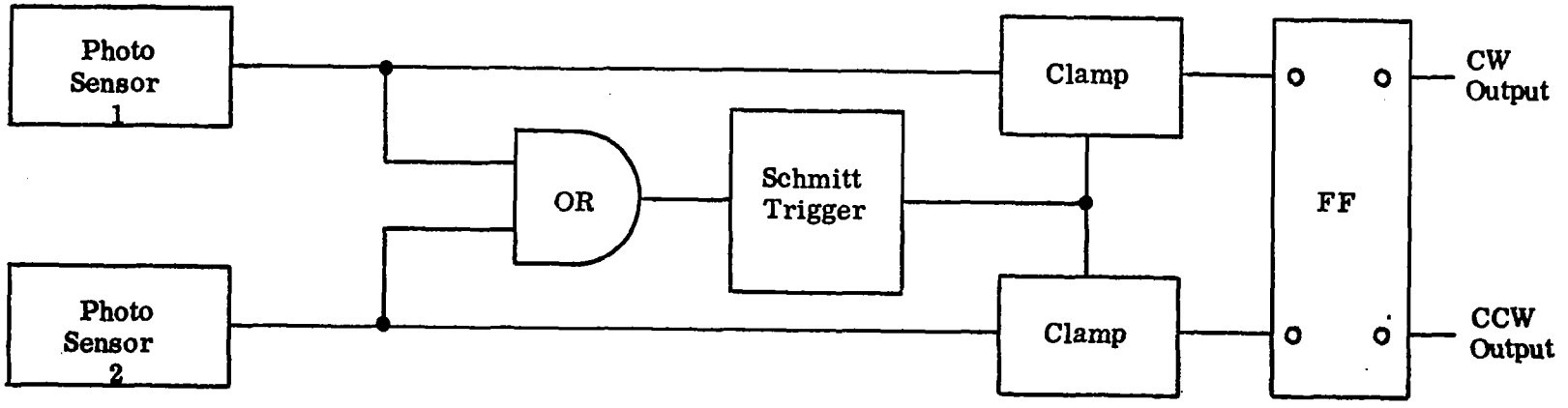

FIGURE 5
BLOCK DIAGRAM OF ROTATION SENSING CIRCUIT

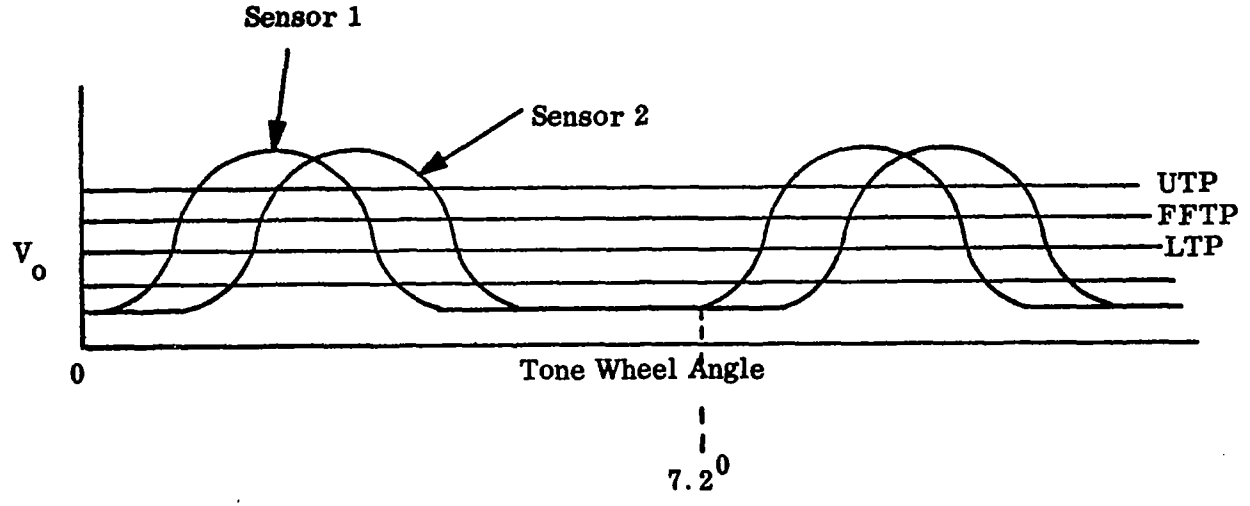

FIGURE 6
SENSOR OUTPUT VOLTAGE VS. TONE WHEEL ANGLE

sensors, both outputs are below the LTP. The FF is then ready to be reset by the sensor that is illuminated first. If the direction of rotation does not change, the FF state remains the same. This relationship is shown by Figure 6. With this system the maximum rotation the inertia wheel can make without its direction of rotation being indicated is the angle between slot centers on the tone wheel which is $7^0 12''$.

F. TACHOMETER

The wheel velocity was determined by an electronic tachometer. The tachometer utilizes the same photosensors, light source, tone wheel, and Schmitt trigger that are used in the rotation direction detector. The output of the Schmitt trigger is differentiated and used to drive a monostable multivibrator whose output is then integrated to provide a DC voltage proportional to wheel velocity. An emitter follower output stage provides an output impedance of less than 100 ohms. The tachometer circuit for reaction wheel number three is shown in Figure 7. The output voltage E_o is greater than 10V at 250 RPM.

The maximum output voltage of the tachometer is 15.5 volts. Without compensation, this occurs at approximately 400 RPM. At this point the monostable is being operated at its maximum repetition rate. A further increase in the trigger rate results in the monostable triggering on alternate pulses which drops the output voltage to approximately 8 volts.

Since the maximum no-load speed of the reaction wheel (unit 3) is near 400 RPM, compensation was added to the tachometer to prevent the maximum repetition rate from being exceeded. A 21-volt zener diode was added to provide feedback from the tachometer output to the base of the monostable output transistor to

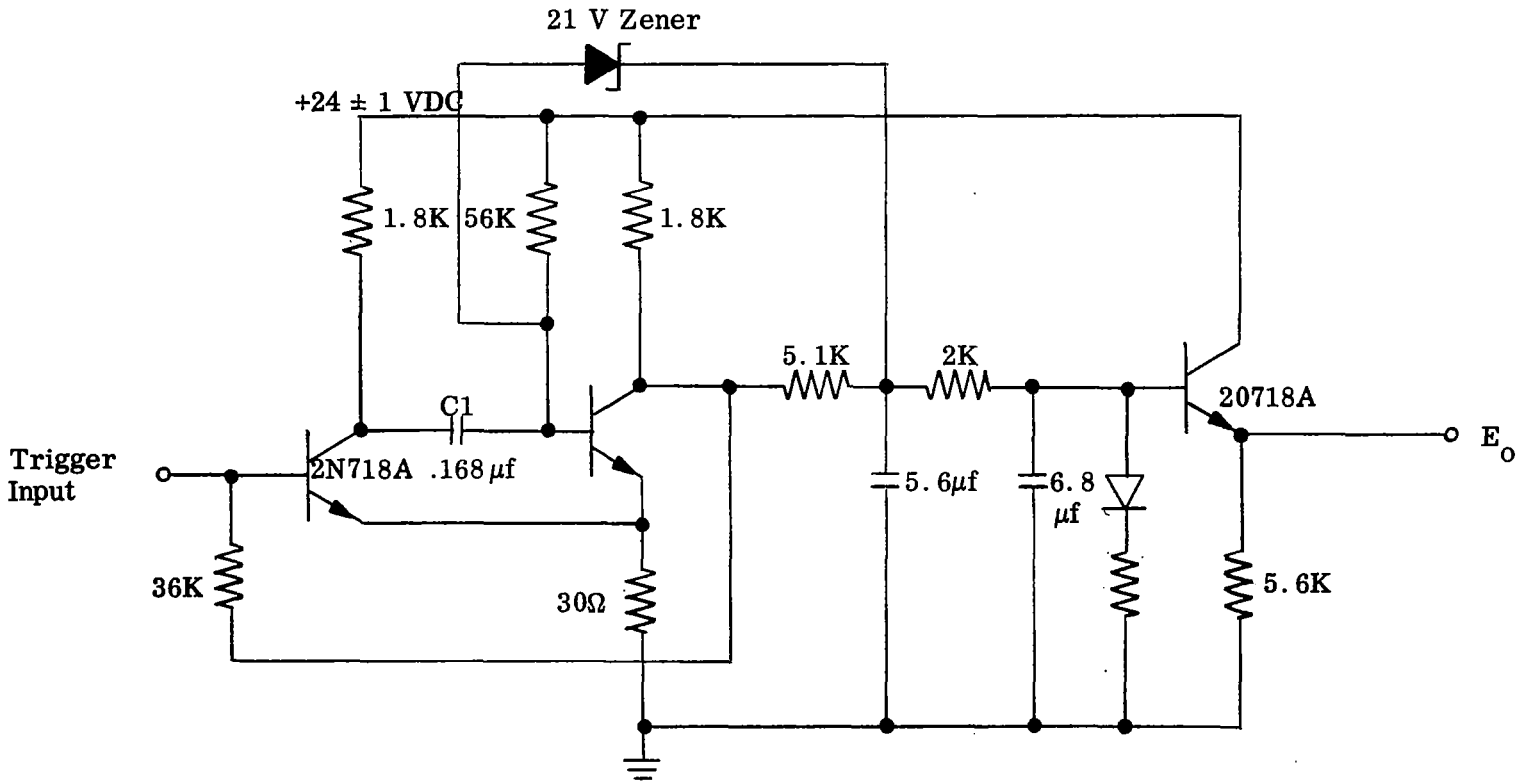

FIGURE 7
TACHOMETER CIRCUIT

reduce the time period. The feedback occurs only when the output is above 10 volts so that the output linearity from 0 to 10 volts is not disturbed. With feedback, the maximum repetition rate occurs at 600 RPM, a value the reaction wheel will not reach.

Tachometer output voltage under voltage and temperature extremes is shown in Figure 8. Approximately 1% of the variation is caused by the power supply change, the remainder is due to the temperature variation. The transistors in the monostable multivibrator produce the largest amount of the tachometer output voltage variation with temperature. The use of a temperature compensated capacitor (C1) in the monostable reduces the variation due to this component to a negligible amount. The output voltage is proportional to speed within 5% from 10% of the unload wheel speed to the unload speed.

The unload speed of unit three is 250 RPM and for unit four it is 400 RPM. In unit four, C1 was reduced to . 08 μf to reduce the output pulse width of the monostable multivibrator and thus reduce the tachometer output voltage to 10 volts at 500 RPM.

G. BI-DIRECTION

In units one and two, the direction of rotation was controlled by applying +24 VDC to the appropriate set of photosensors. The revised specification called for units 3 and 4 to be controlled by a +4 VDC control signal. The circuit shown in Figure 6 of the April, 1965 progress report provides a 24-volt supply to the desired set of photosensors upon the receipt of a 4 VDC input. With no input command, Q16 and Q17 are both off. When an input command is applied to point 1, Q16 turns on and provides Q17 a base current path and causes Q17

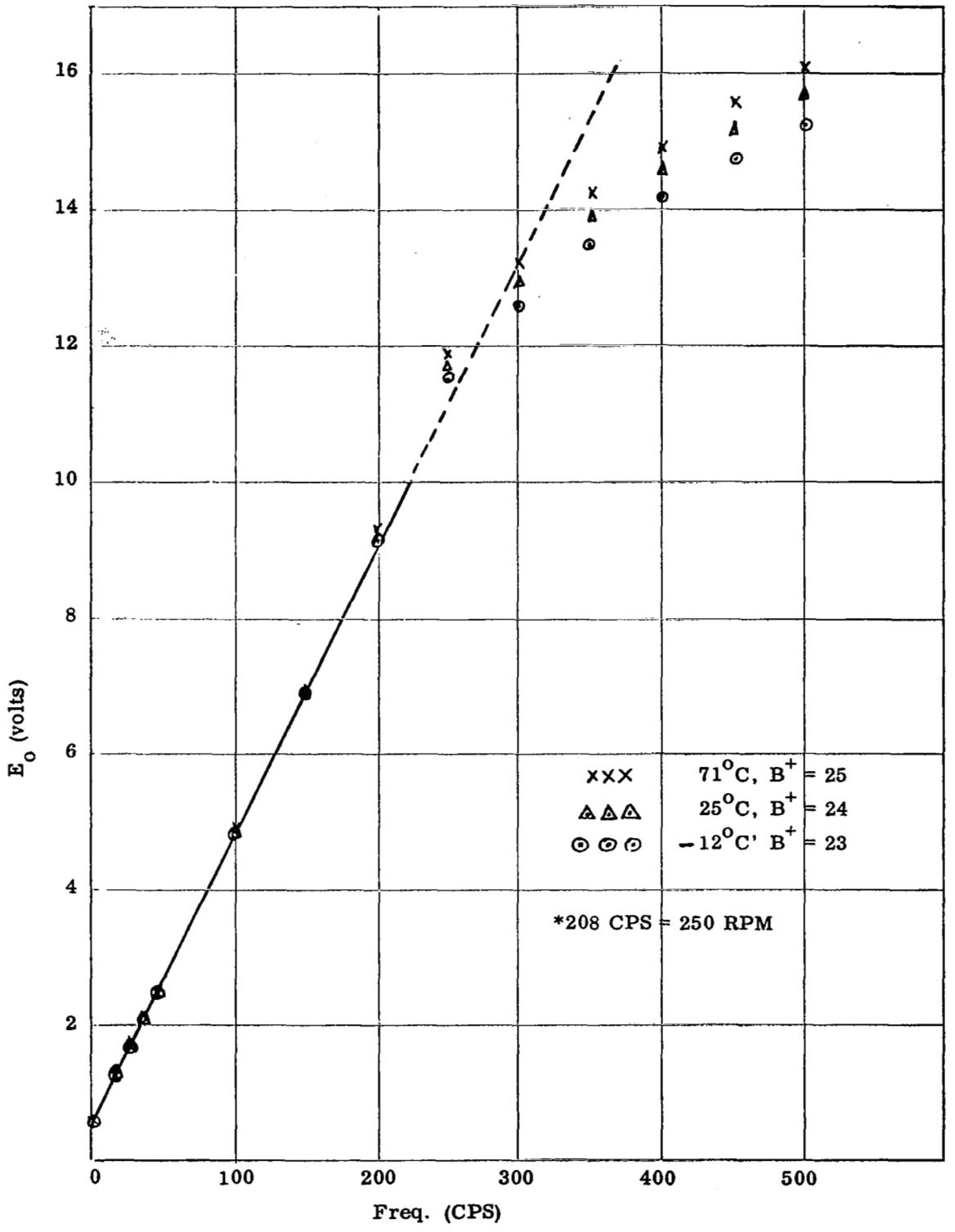

FIGURE 8
TACHOMETER OUTPUT - TEMPERATURE AND VOLTAGE EXTREMES

to conduct. Q17 saturates and applies 24 V to the clockwise set of photosensors. CR7 prevents Q16 from turning on if some small leakage current flows into the base. If a command is applied to point 2, power is applied to the counterclockwise set of photosensors.

H. REGENERATIVE BRAKING

A rotating inertia wheel contains some kinetic energy which must be dissipated if the direction of rotation is to be reversed. When the appropriate set of photosensors is energized to reverse the motor, maximum armature current flows until the wheel has decelerated to 0 RPM and accelerated to a speed determined by the constant torque level in the opposite direction. Power is being drained from the power supply for this entire cycle. If the energy stored in the rotating inertia wheel can be used to decelerate the wheel for any portion of the speed range, e.g., 250 RPM down to 100 RPM, power drain from the flight system can be reduced. SFCo has developed a system defined as "regenerative braking" which utilizes the counter emf generated in the motor windings to provide the armature current when deceleration of the wheel is required.

A block diagram of the system used in reaction wheels 3 and 4 is shown in Figure 9. When a rotation direction command is received, it is compared to the digital direction of the rotation signal provided by the system to determine if deceleration is required. If deceleration is required, the logic circuitry switches the system from the "driving mode" to "braking" by inhibiting the current from flowing through the driver transistor of the upper switches. The armature current is now driven by the generated voltage through the lower commutating switches (1, 3, and 5) through the "Brake driver" stages of the

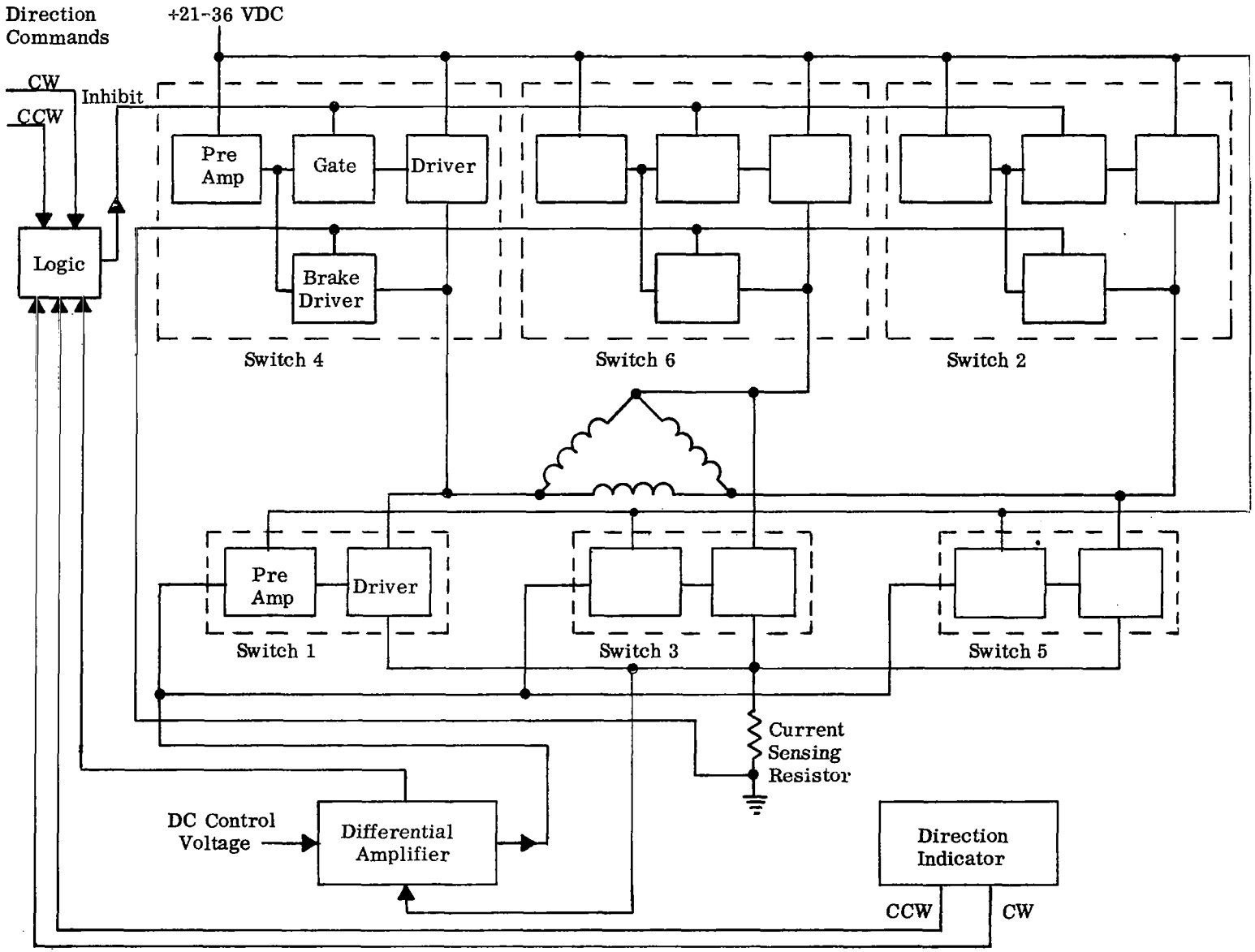

FIGURE 9
REACTION WHEEL SYSTEM WITH REGENERATIVE BRAKING

upper commutating switches (2, 4, and 6). When the system is switched into the regenerative "braking" mode, the "braking" current that begins flowing through the armature is sampled to determine if it is equal to the current commanded by the differential amplifier which controls the current limiter. If the current is sufficient, the system remains in the "braking" mode but if the current is not sufficient, the logic circuitry switches the system back into the "driving" mode by removing the inhibit signal from the "driving" switches.

When the system is in the "braking" mode, the wheel velocity decreases and the counter emf decreases with the velocity. When the counter emf decreases such that it can no longer produce the required armature current, the system is automatically switched back into the "driving" mode to maintain constant torque. The armature current is limited by the same set of current limiters in both the "driving" and regenerative "braking" modes of operation. With this type of braking, the armature current is being commutated and limited at all times regardless of whether the system is "driving" or "braking."

The commutator circuit diagram and the regenerative braking circuit are shown in ENG 10131, the schematic diagram for unit three. "And" gates with inputs from the reaction wheel direction indicator and external direction commands are used to determine when deceleration of the wheel is required. These "And" gates consist of CR1, CR2, CR5, CR6, R1, and R4.

When the command and direction indicator inputs are in agreement, the positive inputs at either gate saturate transistor Q2 of the Schmitt trigger which turns Q1 "off."

When the direction command is reversed, Q2 is turned to the "off" state turning Q1 "on" which produces a negative going voltage at the Q1 collector. This voltage is coupled through capacitor C1 to the base of Q10 turning it "off" and setting the brake-drive flip-flop, comprised of Q10 and Q11, to the "brake" position. In the "brake" position Q12 is biased "on" which in turn switches Q13 "on." Q13 conducts and reverse biases the base-emitter junctions of Q33, Q40, and Q26 which inhibits motor current from flowing through the main driving transistors Q36, Q41, and Q27. Pre-amp current is still being supplied to the "brake" driver transistors Q35, Q42, and Q28. Armature current now flows through the windings; the lower driver transistors Q24, Q31, and Q38; the current sensing resistors R84, R85 and back through Q35, Q42, and Q28. When the generated voltage is no longer sufficient to provide the required current, the current through R84 and R85 decreases, the differential amplifier senses the decrease through R84 and tries to increase the current. The differential amplifier thus drives Q17 into saturation. The Schmitt trigger comprised of Q15 and Q16 detects this saturation voltage (after it is filtered by C14 and R59) and the Schmitt turns off. This drops the collector voltage on Q15 and turns on Q14 which turns on Q10 and switches the flip-flop back to the "Drive" position which turns off Q13 to allow the main motor current to flow again.

The capacitor C1 must be of sufficient size to insure that the flip-flop is held in the brake position for approximately 70 ms. This allows the output from the differential amplifier to indicate if the generated current is of sufficient magnitude to satisfy the control input requirements.

After the turn off voltage to the flip-flop decays, the position of the flip-flop is determined by the output from Q14. At any time the commutator current

does not meet the control input requirements the differential amplifier output saturates, turning the brake-drive flip-flop to the drive position through transistors Q16, Q15, and Q14. DC coupling has been used between the differential amplifier and the brake-drive flip-flop to insure that the flip-flop will stay in the drive position when the commutator current is below the input requirement.

The braking logic circuitry is further explained in the monthly progress report for May, 1965. Regenerative braking is explained also in the progress reports for March, April, and May of 1965.

I. MECHANICAL DESIGN OF REACTION WHEELS

The stator holder, an inseparable part of the housing, was partially machined as a separate detail to obtain an air gap between the bearing seat and stator holder. The air gap minimized the heat transfer by conduction from the stator to the bearings. The stator holder was pressed into the housing and pinned in place.

Ribs and webs were machined in the base of the housing and cover to obtain maximum strength and minimum weight. The housing and cover were supported in the center with a stud to prevent the unit from collapsing when subjected to an internal vacuum during purging and to strengthen the unit during vibration and shock.

Units three and four were sealed by soldering the housing to the cover using an interconnecting solder ring. The solder ring enables the disassembly process, since it is not required to bring the entire solder joint up to the melting point of solder at the same time.

The 7075 T6 aluminum housing, cover and ring on unit number one was plated with gray nickel for solderability. The mating diameters on the cover and housing were machined after plating to prevent the overflow of solder from the cover to the housing. During machining the plating pealed from the housing and unit number one was not sealed. The solder areas on units two, three, and four were tin-lead plated. The tin-lead plating on unit two was masked off and the remaining surfaces were black anodized. Unit two was not sealed. The detail parts on units number three and four were alodined. The units were not black anodized after assembly as planned because of the danger involved in breaking the hermetic seal and damaging the internal parts. Units three and four were purged to 1/2 atmosphere of 90% nitrogen and 10% helium and sealed.

The four flywheels were balanced to 1000 microinch ounces of unbalance. The webs on units two, three, and four were removed and the deflection increased 43 percent. Teflon stops were added to the cover on unit number four to prevent the flywheel from damaging the cover during vibration and shock.

The stators and rotors on units three and four were pinned in place to prevent movement during vibration and shock.

The lamp and sensor assembly for units three and four was redesigned to increase the output of the sensors to eliminate one of the pre-amp transistors in the commutator circuit. The sensor output was increased by mounting the lamps vertically on a reflective surface and reducing the distance between the lamps and sensors.

SECTION IV

PERFORMANCE CHARACTERISTICS

This section describes the achieved performance characteristics of the four reaction wheel systems.

A. UNITS ONE AND TWO

Since unit two is like unit one, only the characteristics of unit one will be covered here.

1. Speed Torque

The data for the speed torque curve for these two units is shown in Table 1 and the curve is shown in Figure 10. The slope of the curve in the desired constant torque region was caused by the increase in rotational losses with speed and by the nonlinearity of the open loop current limiting as the voltage across the limiting transistor changes with wheel velocity.

Speed RPM	Current Amps	Torque Ft. Lb.
346	0.172	0
303	0.55	0.184
267	0.91	0.323
255	1.11	0.365
247	1.07	0.394
216	1.2	0.460
100	1.26	0.490
57	1.275	0.500
0	1.28	0.519

TABLE 1
SPEED TORQUE DATA FOR UNIT ONE

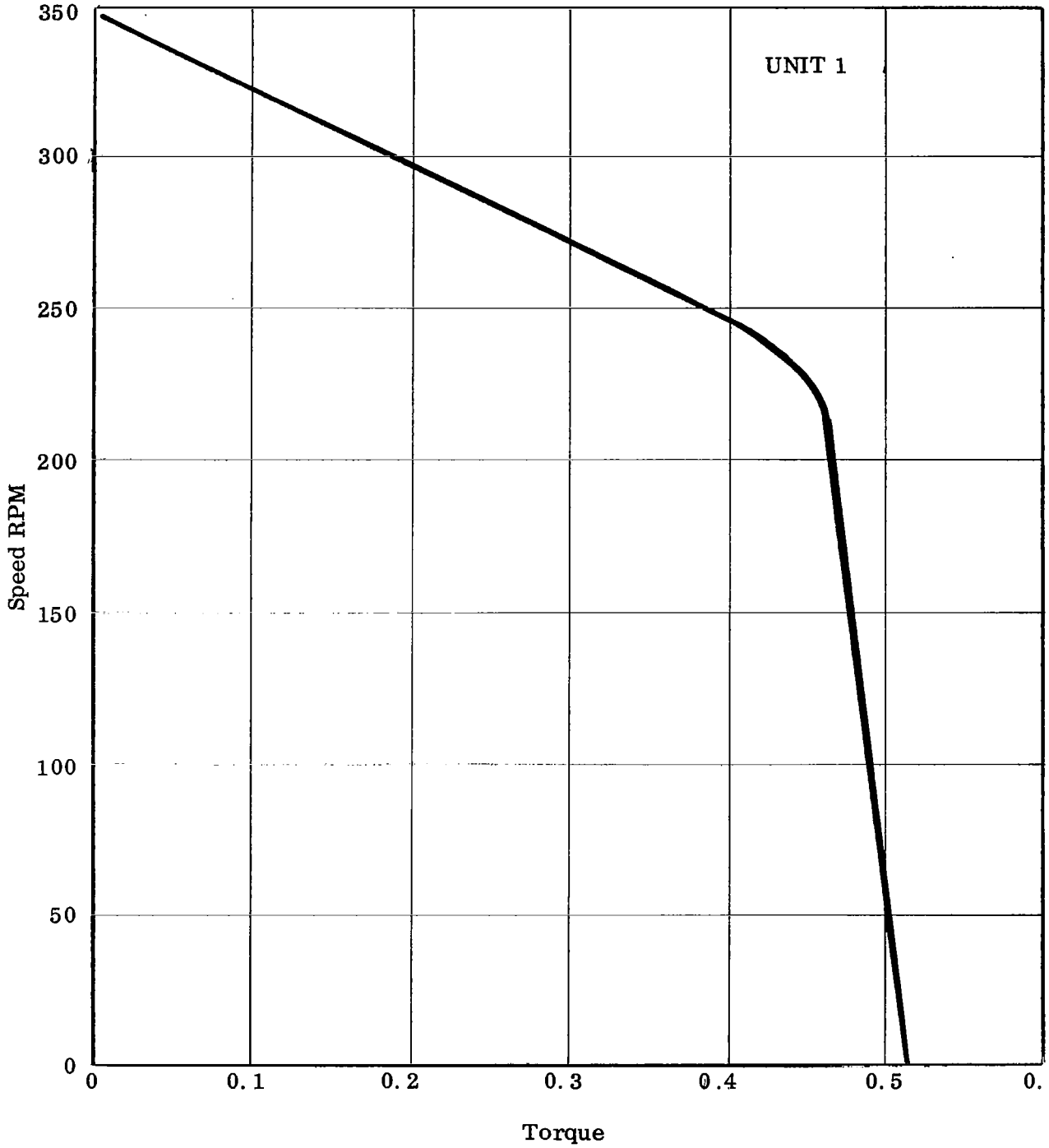

FIGURE 10
SPEED TORQUE CURVE

2. Other characteristics of units one and two are listed below.

   a. Inertia - 1.25 lb. ft.^{2}

   b. Momentum - 4.0 lb. ft. sec. at 1000 RPM
      1.0 lb. ft. sec. at 250 RPM

   c. Speed - 1260 RPM max.

   d. Power Input - 30.7 watts max.

   e. Voltage - 24 VDC

   f. Weight - 12.5 lbs.

   g. Size - 12" x 12" x 4"

   h. Ripple torque - +6.64%
      -14.7%

   i. DC Control Voltage - 0-12 VDC (Response plotted in Figure 11)

   j. DC tachometer voltage proportional to speed (Response plotted in Figure 12)

   k. Friction - .033 ft. lb.

   l. Hermetic sealing portion of the specification was waived.

   m. Both units are bidirectional.

   n. Vibration and shock tests of these two units were waived.

   o. Both units performed satisfactorily over temperature range of -10^{o}C to +70^{o}C.

B. UNITS THREE AND FOUR

1. Speed Torque

The data for the speed torque curve for unit three is shown in Table 2 and is plotted in Figure 13. The closed loop current limiting used in units three and four solved the nonlinearity problem of the current limiting and thus a more constant speed torque was obtained. The data for the speed torque curve for unit four is shown in Table 3 and is plotted in Figure 14.

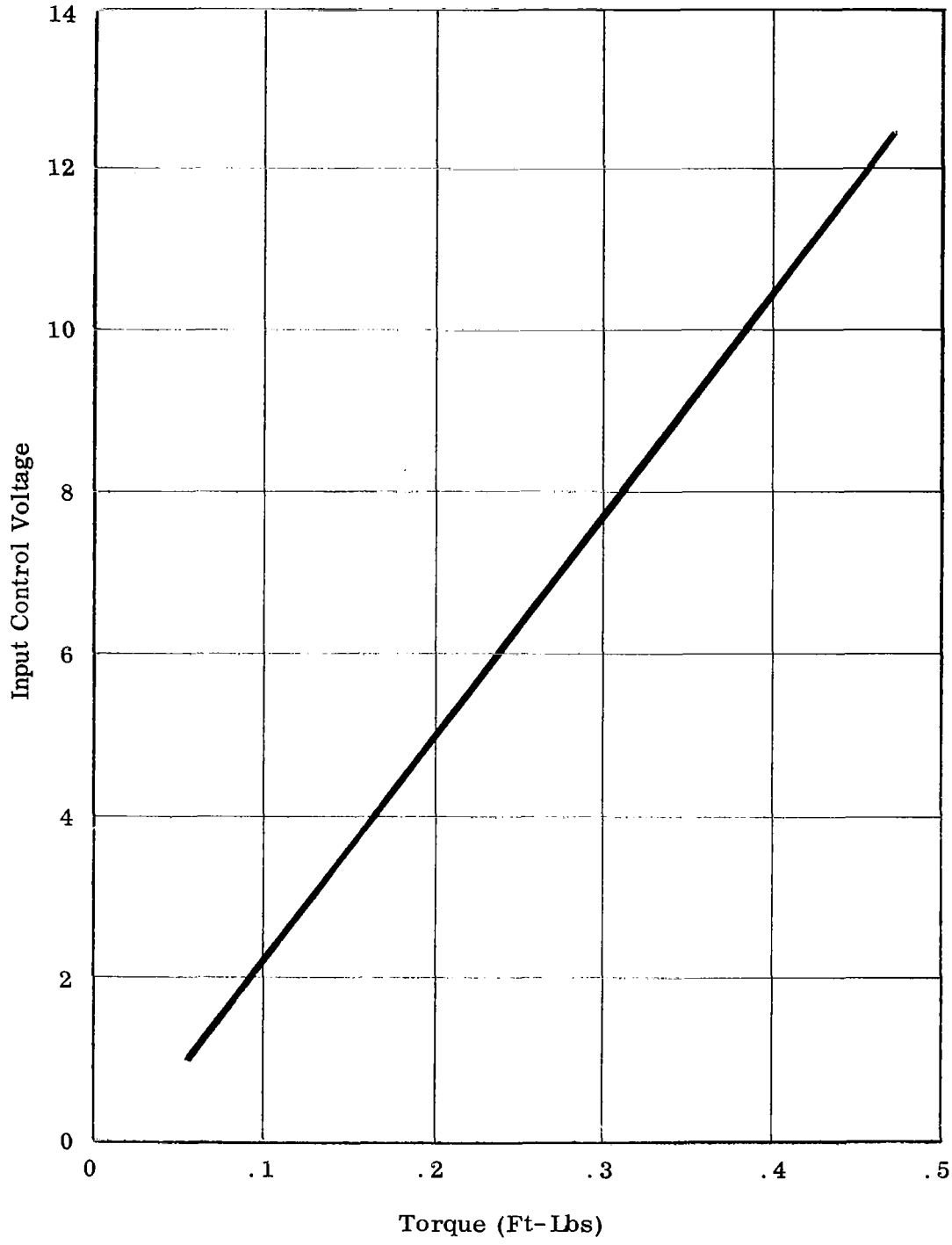

FIGURE 11
STALL TORQUE VS DC CONTROL VOLTAGE INPUT UNIT 1

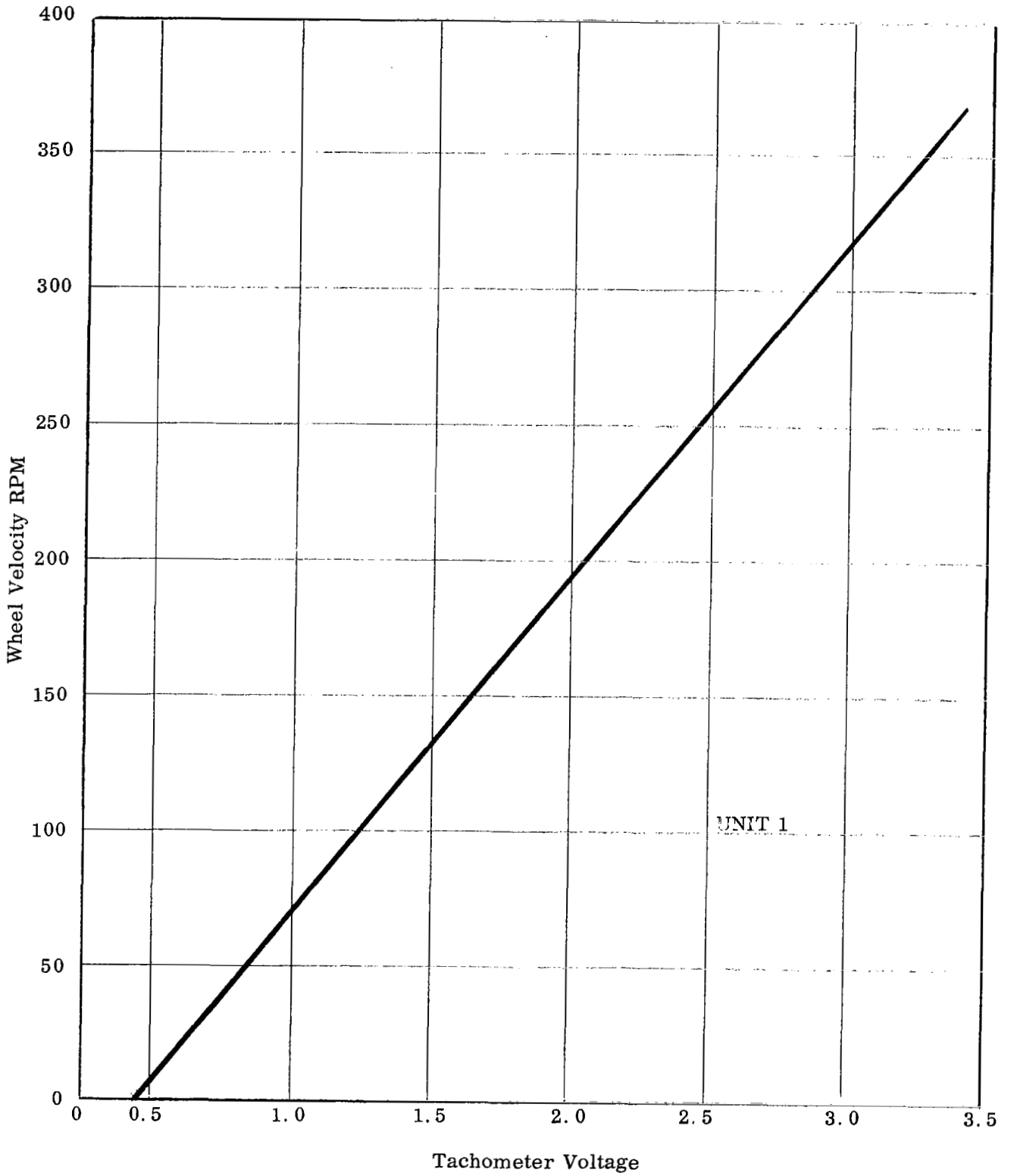

FIGURE 12
TACHOMETER OUTPUT VOLTAGE VS WHEEL VELOCITY

Volts Applied	RPM	Torque Ft. Lb.	Line Current (Amps)
21	327	0	0.15
21	266	0.285	0.81
21	221	0.511	1.315
21	210	0.562	1.435
21	191	0.637	1.618
21	115	0.649	1.637
21	39	0.651	1.64
24	375	0	0.165
	312	0.286	0.825
24	267	0.51	1.33
24	250	0.598	1.52
24	244	0.625	1.59
24	240	0.637	1.615
24	212	0.64	1.635
24	187	0.646	1.64
24	103	0.65	1.645
24	50	0.65	1.645
24	26	0.65	1.645
36	568	0	0.21
36	495	0.294	0.885
36	443	0.529	1.41
36	412	0.614	1.59
36	275	0.638	1.64
36	63	0.644	1.643

TABLE 2
SPEED TORQUE DATA, UNIT THREE

Reaction Wheel # 3

1 = 21V
2 = 24V
3 = 36V

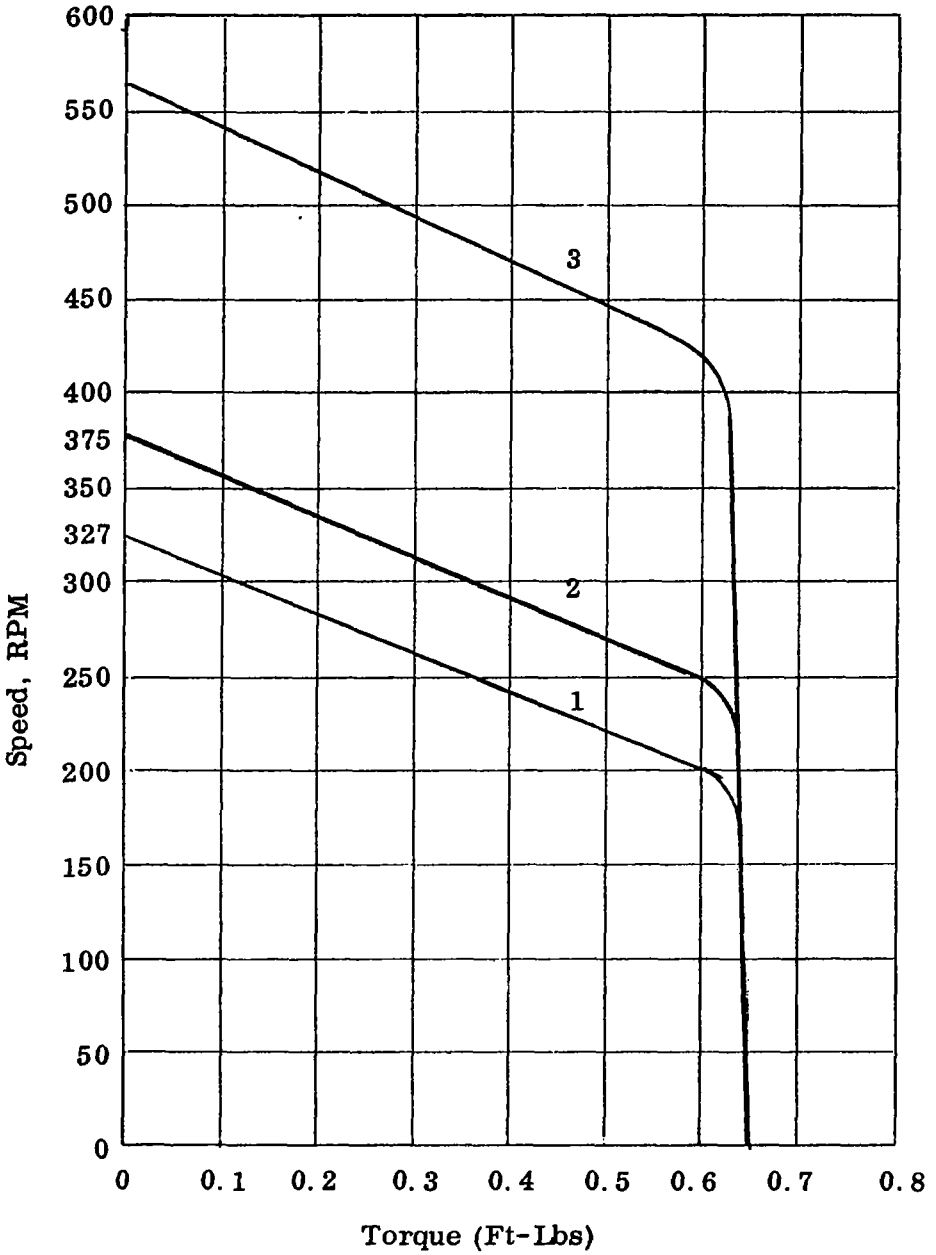

FIGURE 13
SPEED TORQUE CURVE

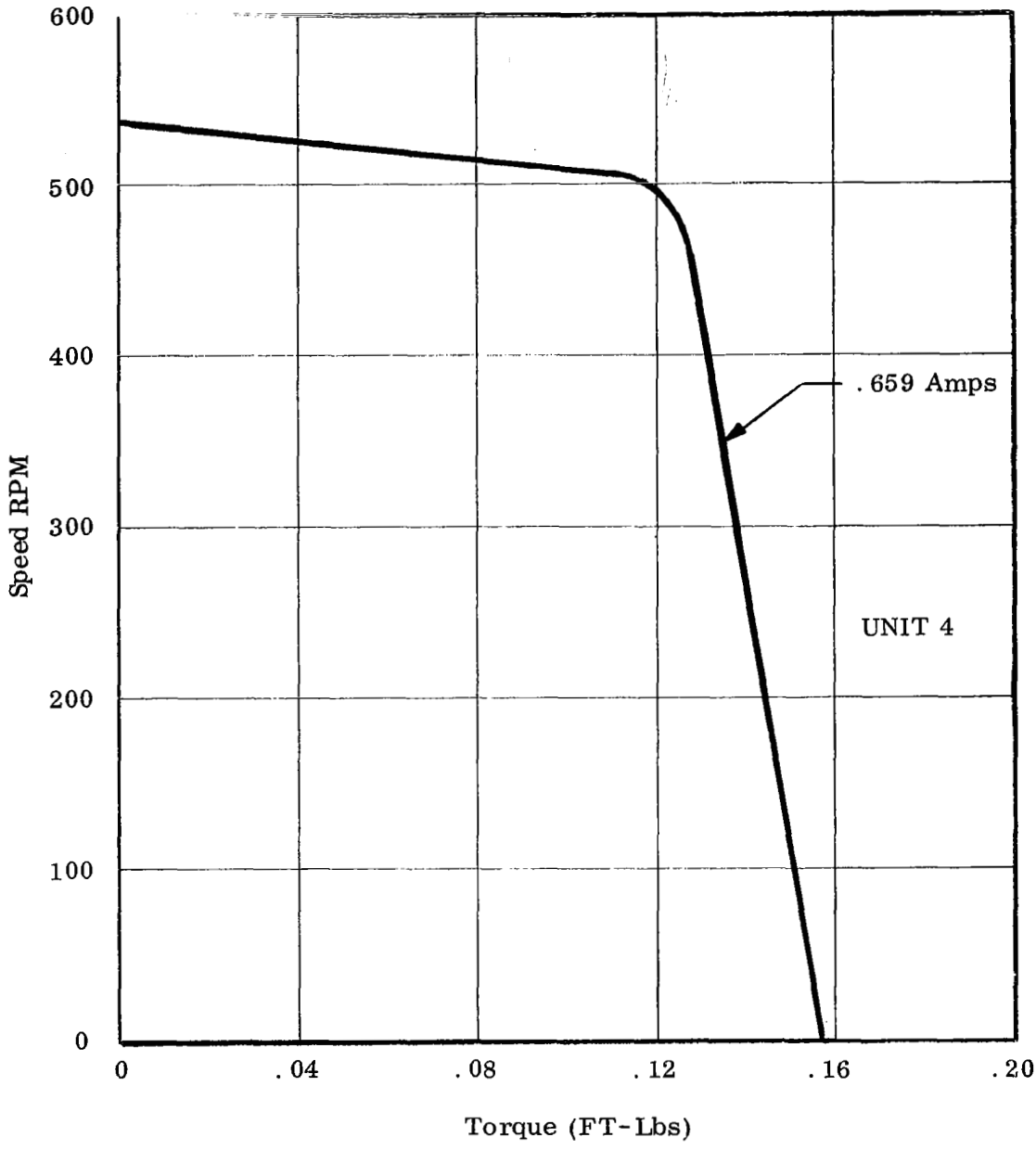

FIGURE 14
SPEED TORQUE CURVE

2. Other characteristics of units three and four are listed below.

   a. Inertia - 1.25 lb. ft.^{2}

   b. Momentum - 1.0 lb. ft. sec. @ 250 RPM
      2.0 lb. ft. sec. @ 500 RPM

   c. Power Input - 40 watts max. (unit three)
      16 watts max (unit four)

   d. Voltage - Operate over voltage range of 21 to 36 VDC

   e. Weight - 13.7 lbs.

   f. Size - 12" x 12" x 3"

   g. Ripple Torque - +5.72%
      -12.1%

   h. DC Control voltage - 0-4 VDC (Response plotted in Figure 15)

   i. Tachometer voltage proportional to speed. (Response plotted in Figure 16)

   j. Both units are hermetically sealed per Specification 67-33, Revision A.

   k. Both units are bidirectional.

   l. Both units have "regenerative" braking.

   m. Per request of GSFC, unit four was subjected to the vibration and shock tests but unit three was not. The unit was exposed to 50 g shock of 8 ms duration, and 5 minutes of 15 g rms sinusoidal vibration in each of three perpendicular planes.

   n. Both units perform satisfactorily over the specified temperature range of 10°C to $+70^{\circ}$C.

   o. Friction - 0.023 ft. lb.

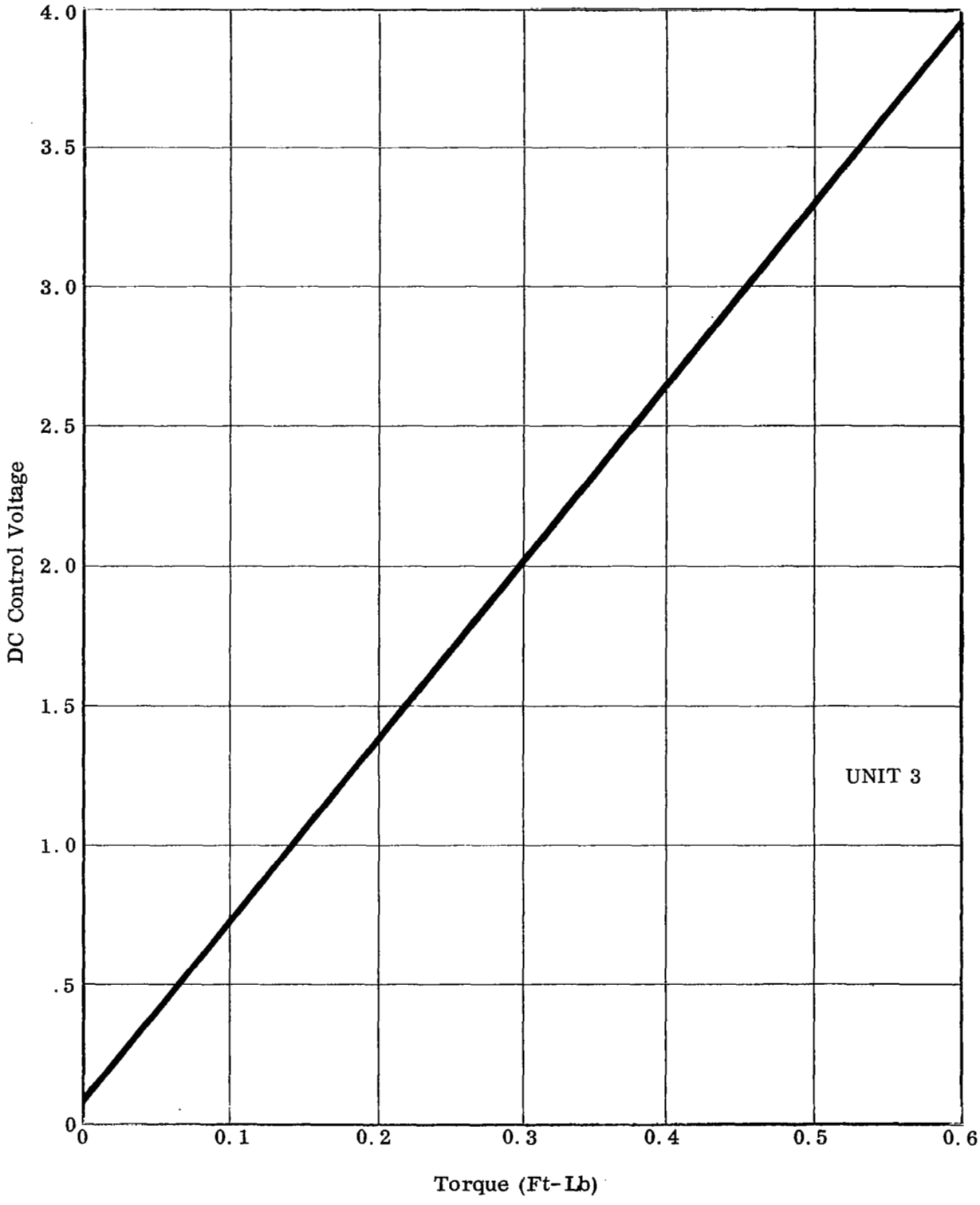

FIGURE 15
OUTPUT TORQUE VS DC CONTROL VOLTAGE

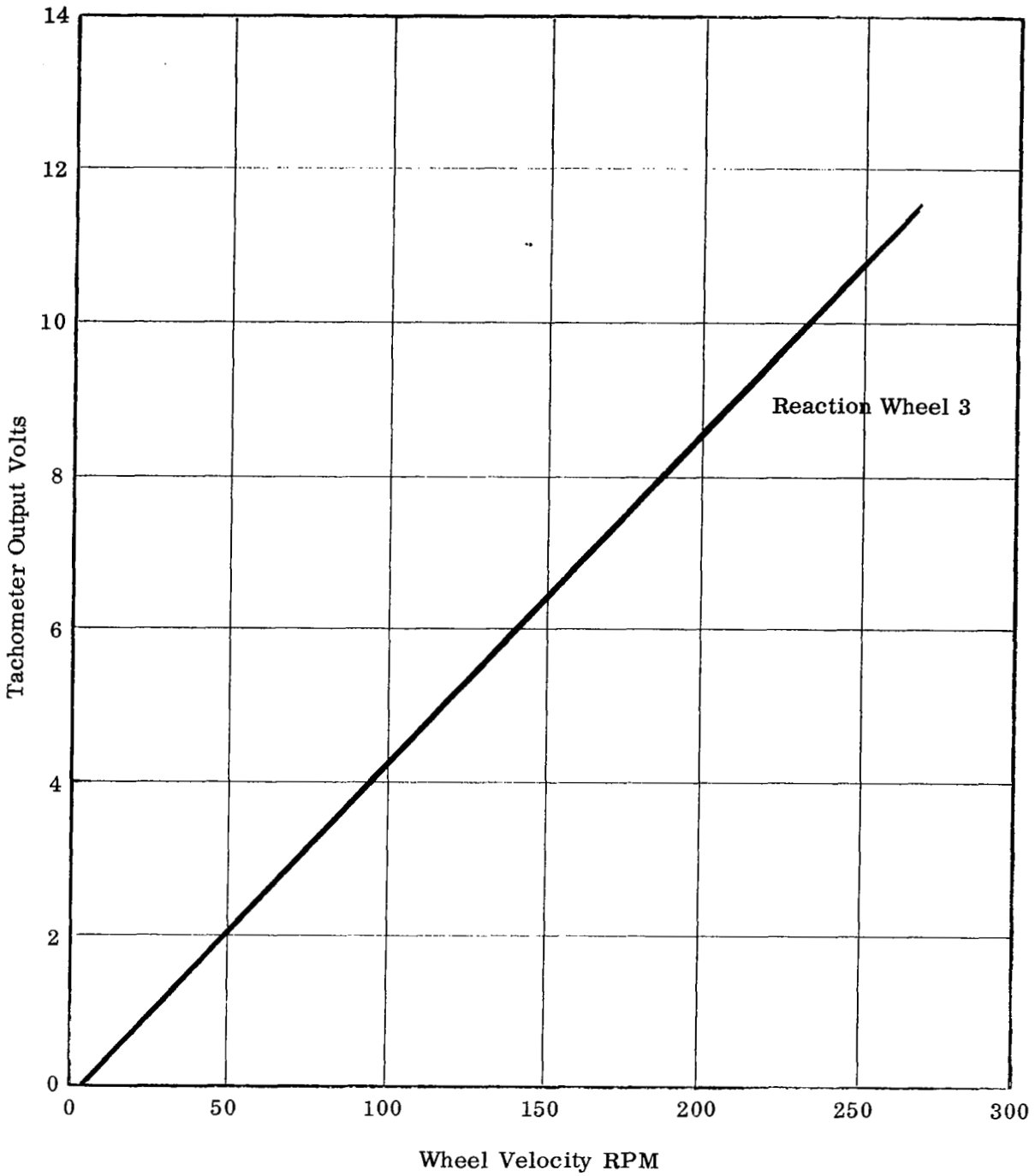

FIGURE 16
TACHOMETER OUTPUT VOLTAGE VS WHEEL VELOCITY

Speed RPM	Current Amps	Torque Ft. Lb.
537	0.255	0
520	0.45	0.06
504	0.635	0.115
461	0.659	0.127
356	0.659	0.132
275	0.659	0.137
200	0.659	0.142
141	0.659	0.147
66	0.659	0.152

TABLE 3
SPEED TORQUE DATA, UNIT FOUR

C. RELIABILITY

1. Production Unit Three

The failure rate and predicted reliability for each section of reaction wheel number three as delivered to GSFC are shown in Table 4. The calculations are based on the unit operating at the following power levels:

* 1 percent of the time at peak power
* 5 percent of the time at 50 percent of peak power
* 94 percent of the time at 6.9 percent of peak power

The average power level is 10 percent of peak power. The reliability predictions were made using MIL-HDK-217 failure rates and considering all parts in series and assuming any part failure to be a complete system failure. The predictions include the motor windings and circuit boards. The predicted reliability of unit three is 98% for 1000 hours, 83.9% for 1 year, and 59.1% for 3 years. The predicted reliability for the motor and commutator for 1 year is 93.6% and for 3 years is 82 percent. The failure rate for each component of unit three is included in Appendix I.

The four diodes in parallel with each lamp prevent a higher voltage across the other six lamps in case of a lamp failure. Since the failure of one lamp is being viewed as a total system failure, the failure rates of diodes CR70 through CR97 are not considered as decreasing the reliability of the system.

Section	Failure Rate Percent Per 1000 Hrs.	Predicted Reliability 1 Year	3 Years
Motor and Commutator	0.7569	93.6	82.0
Regenerative Braking	0.2180	98.2	94.74
Direction Indicator	0.1798	98.55	95.8
Tachometer	0.1644	98.4	95.3
Differential Amplifier	0.2512	97.8	93.6
Logic and Command Circuits	0.4295	96.3	89.35
TOTAL	1.9998	83.9%	59.1%

TABLE 4
RELIABILITY PREDICTIONS FOR UNIT THREE

2. High Reliability Unit

By using high reliability parts where significant reductions in failure rates could be achieved and by using burned-in and x-rayed semiconductors, the failure rates and predicted reliability figures shown in Table 5 were calculated.

The predicted reliability of 87.2% for the motor and commutator for three years shows that a significant increase in reliability can be obtained by using high reliability parts. The predicted figure for the complete reaction wheel to operate for three years without any failures has been increased to 71 percent.

Section	Failure Rate Percent Per 1000 Hrs.	Predicted Reliability 1 Year	3 Years
Motor and Commutator	.5166	95.5	87.2
Regenerative Braking	.1430	98.75	96.3
Direction Indicator	.1248	98.95	96.77
Tachometer	.0940	99.15	97.6
Differential Amplifier	.1614	98.5	95.8
Logic and Command Circuits	.2625	97.7	93.0
TOTAL	1.3023	89.2%	71.0%

TABLE 5
RELIABILITY PREDICTION USING HIGH RELIABILITY PARTS

APPENDIX I

RELIABILITY ANALYSIS OF REACTION WHEEL NUMBER THREE

ENG 10126

Item	Schematic Symbol	Description	Failure Rate
1	A1-A12	Photosensor	.120
2	CR24,25,40,41,42,43, 51,52,56,57,29,30	Diode	.0228
3	R99,111,86	Resistor	.003
4	R100,112,87	Resistor	.003
5	CR44, 58, 31	Diode	.030
6	Q32,39,25	Transistor	.060
7	R101,113,88	Resistor	.003
8	R102,114,89	Resistor	.003
9	R103,115,90	Resistor	.003
10	Q33,40,26	Transistor	.060
11	R134,116,91	Resistor	.003
12	Q34,41,27	Transistor	.060
13	CR46,47,62,63,33,34	Diode	.030
14	R82,96,108	Resistor	.003
15	Q23,37,30	Transistor	.060
16	R83,98,109	Resistor	.003
17	Q24,31,38	Transistor	.060
18	R131,97,110	Resistor	.0048
19	R85,84	Resistor	.032
20	DS1-DS7	Lamp	.0136
21		Windings	.075
22	CR67	Diode	.010

TABLE I-1
COMMUTATOR FAILURE RATE

TABLE I-1 (CONT.)

Item	Schematic Symbol	Description	Failure Rate
23	R132	Resistor	.001
24	Q44	Transistor	.020
25	R121	Resistor	.0027
26	R122	Resistor	.001
27	Circuit Cards	Circuit Cards	.070
	Component failure rate, per cent/1000 hours		.7569

$R = e^{-\lambda t}$

$R = e^{-.7569 \times 8,760 \times 10^{-5}}$

R = 93.6% for t = 1 year.

R = 82% for t = 3 years.

Item	Schematic Symbol	Description	Failure Rate
1	CR45,59,32	Diode	.0057
2	CR98,61,37	Diode	
3	CR36,60,99	Diode	
4	R105,118,93	Resistor	.003
5	R106,119,94	Resistor	.003
6	Q36,43,29	Transistor	.060
7	CR48,64,35	Diode	.030
8	R107,120,95	Resistor	.0033
9	R104,117,92	Resistor	.003
10	Q35,42,28	Transistor	.060
11	CR49,50,65, 66,38,39	Diode	.030
12	Circuit Card	Circuit Card	.020
13	CR26,27,28,53,54, 55,100,101,102	Diode	
	Component failure rate, per cent/1000 hours		0.2180

$R = e^{-\lambda t}$

$R = e^{-.2180 \times 8,760 \times 10^{-5}}$

R = 98.2% for t = 1 year.

R = 94.74% for t = 3 years.

TABLE I-2
REGENERATIVE BRAKING FAILURE RATE

Item	Schematic Symbol	Description	Failure Rate
1	A13, 14	Photosensor	.020
2	R24, 25	Resistor	.002
3	CR8, 9	Diode	.0038
4	CR10	Diode	.010
5	R17	Resistor	.001
6	R16	Resistor	.001
7	C4	Capacitor	.002
8	R15, 23	Resistor	.002
9	CR7, 11	Diode	.0038
10	Q5	Transistor	.020
11	R18	Resistor	.0016
12	R27	Resistor	.001
13	R133	Resistor	.001
14	C6	Capacitor	.002
15	Q6	Transistor	.020
16	R28	Resistor	.0016
17	R26	Resistor	.001
18	R14	Resistor	.001
19	R13	Resistor	.001
20	Q4	Transistor	.020
21	R21	Resistor	.001
22	R22	Resistor	.001

TABLE I-3
DIRECTION INDICATOR FAILURE RATE

TABLE I-3 (CONT.)

Item	Schematic Symbol	Description	Failure Rate
23	R19	Resistor	.001
24	C3,5	Capacitor	.004
25	R12,20	Resistor	.002
26	R11	Resistor	.001
27	Q3	Transistor	.020
28	R135	Resistor	.001
29	Circuit Card	Circuit Card	.033
	Component failure rate, per cent/1000 hours		0.1798

$R = e^{-\lambda t}$

$R = e^{-0.1798 \times 8760 \times 10^{-5}}$

R = 98.55% for t = 1 year.

R = 95.8% for t = 3 years.

Item	Schematic Symbol	Description	Failure Rate
1	C7	Capacitor	. 002
2	R29	Resistor	. 001
3	CR12	Diode	. 0019
4	R30	Resistor	. 001
5	Q7	Transistor	. 020
6	R31	Resistor	. 001
7	C9	Capacitor	. 001
8	C8	Capacitor	. 001
9	R32	Resistor	. 0011
10	R33	Resistor	. 001
11	CR13	Diode	. 010
12	Q8	Transistor	. 020
13	R38	Resistor	. 0035
14	R34	Resistor	. 001
15	R35	Resistor	. 001
16	C16	Capacitor	. 024
17	C10	Capacitor	. 018
18	CR14	Diode	. 0019
19	R36	Resistor	. 001
20	Q9	Transistor	. 020

TABLE I-4
TACHOMETER FAILURE RATE

TABLE I-4 (CONT.)

Item	Schematic Symbol	Description	Failure Rate
21	R37	Resistor	.001
22	Circuit Cards	Circuit Cards	.032
	Component failure rate, per cent/1000 hours		0.1644

$R = e^{-\lambda t}$

$R = e^{-0.1644 \times 8760 \times 10^{-5}}$

R = 98.4% for t = 1 year.

R = 95.3% for t = 3 years.

Item	Schematic Symbol	Description	Failure Rate
1	R81	Resistor	.001
2	R80	Resistor	.001
3	Q18	Transistor	.020
4	R72, 73	Resistor	.0022
5	C15	Capacitor	.020
6	R74, 75	Resistor	.002
7	Q22	Transistor	.020
8	R78	Resistor	.001
9	R79	Resistor	.030
10	R77	Resistor	.001
11	R76	Resistor	.001
12	R63	Resistor	.001
13	Q21	Transistor	.020
14	Q20	Transistor	.020
15	R71	Resistor	.0012
16	R67	Resistor	.0012
17	R70	Resistor	.001
18	R68	Resistor	.001
19	R69	Resistor	.0025
20	Q19	Transistor	.020
21	R66	Resistor	.0032
22	R61	Resistor	.001

TABLE I-5
DIFFERENTIAL AMPLIFIER FAILURE RATE

TABLE I-5 (CONT.)

Item	Schematic Symbol	Description	Failure Rate
23	R62	Resistor	.001
24	R65	Resistor	.001
25	R64	Resistor	.001
26	R59	Resistor	.001
27	C14	Capacitor	.020
28	Q17	Transistor	.020
29	R60	Resistor	.001
30	CR21,22,23	Diode	.0019
31	Circuit Cards	Circuit Cards	.033
		Component failure rate, per cent/1000 hours	0.2512

$R = e^{-\lambda t}$

$R = e^{-0.2512 \times 8760 \times 10^{-5}}$

$R = 97.8\%$ for $t = 1$ year.

$R = 93.6\%$ for $t = 3$ years.

Item	Schematic Symbol	Description	Failure Rate
1	R58	Resistor	.001
2	R57	Resistor	.001
3	Q15,16	Transistor	.040
4	R52,56	Resistor	.0024
5	R53	Resistor	.001
6	R55	Resistor	.001
7	C13	Capacitor	.002
8	R54	Resistor	.001
9	R51	Resistor	.001
10	Q14	Transistor	.020
11	R50	Resistor	.0019
12	R49	Resistor	.001
13	R39	Resistor	.001
14	R40	Resistor	.0016
15	Q10	Transistor	.020
16	CR16	Diode	.0019
17	C11	Capacitor	.002
18	R42	Resistor	.001
19	C12	Capacitor	.002
20	R44	Resistor	.001
21	CR17	Diode	.010
22	R45	Resistor	.001

TABLE I-6
LOGIC AND COMMAND CIRCUITS FAILURE RATE

TABLE I-6 (CONT.)

Item	Schematic Symbol	Description	Failure Rate
23	R46	Resistor	.001
24	R43	Resistor	.0018
25	Q11	Transistor	.020
26	Q12	Transistor	.020
27	R47	Resistor	.0012
28	R48	Resistor	.001
29	Q13	Transistor	.020
30	CR18, 19, 20	Diode	.0057
31	Q45, 47	Transistor	.040
32	Q48, 46	Transistor	.040
33	R124, 128	Resistor	.002
34	R123, 127	Resistor	.002
35	CR68, 69	Diode	.0038
36	R125, 129	Resistor	.0024
37	R126, 130	Resistor	.002
38	Circuit Card	Circuit Card	.032
39	CR1-6	Diode	.0114
40	R4	Resistor	.001
41	R1	Resistor	.001
42	R2	Resistor	.0022
43	R5	Resistor	.002
44	C2	Capacitor	.002
45	R6	Resistor	.001

TABLE I-6 (CONT.)

Item	Schematic Symbol	Description	Failure Rate
46	Q2	Transistor	.020
47	R8	Resistor	.001
48	R9	Resistor	.001
49	R7	Resistor	.001
50	Q1	Transistor	.020
51	R10	Resistor	.0033
52	C1	Capacitor	.050
53	R3	Resistor	.001
54	CR15	Diode	.0019
		Component failure rate, per cent/1000 hours	0.4295

$R = e^{-\lambda t}$

$R = e^{-0.4295 \times 8760 \times 10^{-5}}$

$R = 96.3\%$ for $t = 1$ year.

$R = 89.35\%$ for $t = 3$ years.

NASA-Langley, 1966 CR-388